LBL-14194
Preprint

Lawrence Berkeley Laboratory
UNIVERSITY OF CALIFORNIA

Accelerator & Fusion Research Division

To be published as an article in Annual Review of Nuclear and Particle Science, Volume 32, Annual Reviews Inc.

INERTIAL CONFINEMENT FUSION

Denis Keefe

March 1982

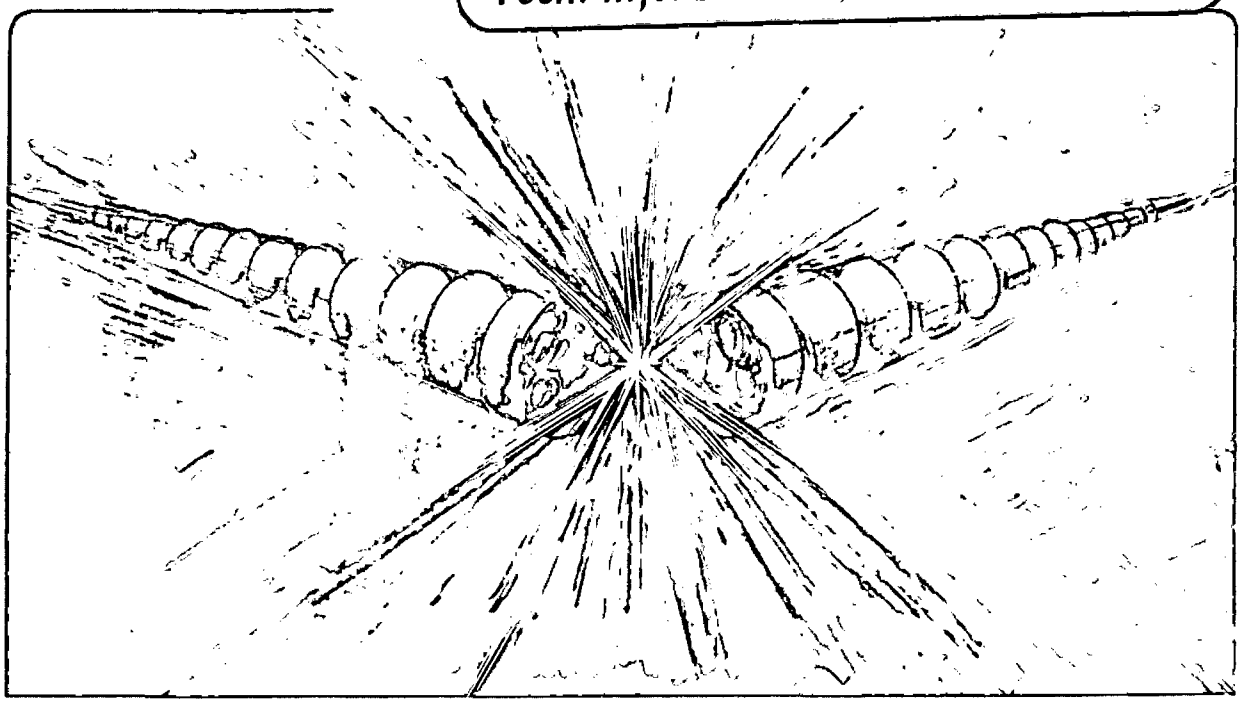

Prepared for the U.S. Department of Energy under Contract DE-AC03-76SF00098

DISCLAIMER

LBL-14194

INERTIAL CONFINEMENT FUSION*

Denis Keefe

Lawrence Berkeley Laboratory

University of California

Berkeley, California 94720

March 1982

* This work was supported by the Assistant Secretary for Defense Programs, Office of Inertial Fusion, Laser Fusion Division, U.S. Department of Energy, under Contract No. DE-AC03-76SF00098.

CONTENTS

1	INTRODUCTION	4
	1.1 Thermonuclear Fusion for Electricity Generation	4
	1.2 The Lawson Criterion for Magnetic and Inertial Confinement	7
	1.3 Inertial Fusion: Advantages and Issues	11
2	PELLET COMPRESSION	14
	2.1 Target Design Considerations	14
	2.2 Energy and Power Needed for Successful Compression	17
3	APPLICATION OF INERTIAL FUSION TO ELECTRIC POWER PRODUCTION	20
	3.1 Target and Driver Requirements	20
	3.2 Reactor Considerations	24
	3.2.1 Single-Pulse Requirements	25
	3.2.2 Repetitive-Pulse Requirements	29
4	LASER DRIVERS FOR INERTIAL FUSION	33
	4.1 Laser Interaction with Matter	33
	4.2 Laser Facilities and Experiments	37
	4.2.1 Available Wavelengths	37
	4.2.2 Short Wavelength Lasers	38
	4.2.3 Long Wavelength Lasers	40
	4.2.4 Advanced Laser Development	43

5 PARTICLE BEAM DRIVERS FOR INERTIAL FUSION 45

5.1 Light Ion Drivers 46

5.2 Heavy Ion Drivers 52

5.2.1 Advantages, Parameters and Issues 52

5.2.2 Accelerator Performance Criteria 56

5.3 Focusing of Ion Beams on the Target 64

6 SUMMARY AND OUTLOOK 68

ACKNOWLEDGMENTS 69

LITERATURE CITED 70

FIGURE CAPTIONS AND FIGURES 77

TABLES 98

1 INTRODUCTION

1.1 Thermonuclear Fusion for Electricity Generation

The attraction of using thermonuclear fusion of light nuclei as a source of electrical energy lies in the small investment needed in the kinetic energy of the ions to achieve a significant number of exothermic fusion reactions each resulting in a very much larger kinetic energy of the reaction fragments. A variety of candidate reactions that have been considered are shown in Table 1 (Dean 1981).

Immediate plans for fusion development rely exclusively on the first reaction, between deuterium and tritium:

$$D + T \rightarrow n + He^4 + 17.6 \text{ MeV}$$

because it requires the least initial energy investment and provides the greatest energy amplification. Despite the theoretically large factor for energy amplification shown in Table 1 much of it will become whittled down by a host of inevitable inefficiency factors in any practical system and by the need to operate at energies substantially above the threshold shown. While "scientific breakeven" experiments are expected to occur within a few years at the Tokamak Fusion Test Reactor (TFTR) at Princeton, it is a long step from that to engineering breakeven (a genuinely energy self-sufficient system) and still a longer one to net output power production. Hence it is natural to concentrate now on the least difficult option--trying to burn deuterium-tritium (D-T) fuel. When that has been successfully

achieved, other more difficult fuel choices would, no doubt, be explored for reactors of a later generation; for example, the D-D reaction, which would avoid the need to breed the radioactive isotope tritium, or the p-B reaction, which produces only charged particles in the final state and so offers the possibility of direct electrical energy conversion without the interpolation of an inefficient thermoelectrical conversion stage.

For fusion to work as a practical source of electricity, physics requires that two conditions be achieved simultaneously for a deuterium-tritium mixture:

1. The temperature should be in the region of $kT = 20$ keV.
2. The hot plasma should be adequately confined; that is, the product, $n\tau$, of the number density, n, and the "confinement time," τ, should lie close to 10^{15} sec cm^{-3}. This corresponds to the so-called Lawson criterion and is discussed in Section 1.2 (Lawson 57).

In short, these conditions will ensure that a sufficiently large number of interactions occur (i.e. enough fuel burned) in the time for which the plasma density and temperature are both adequately high, to produce useful amounts of output energy.

Three methods are known for confinement of thermonuclear plasmas. Gravitational confinement, as in the sun and other stars, is known to be quite successful and to have a long lifetime but, because the confining force of gravity is so weak, has a system scale-length, viz., the solar radius, that is unacceptably large for earthbound

fusion. Systems that use magnetic fields, in either a toroidal or mirror configuration, are being steadily advanced and seem virtually assured of scientific breakeven within a matter of years. For example, the Alcator A tokamak at MIT has already achieved an $n\tau$ product of 3×10^{13} sec cm^{-3}; this would have been adequate for a breakeven demonstration had a hot enough plasma been contained. Finally, inertial confinement refers to the situation where a small volume of thermonuclear fuel--a sphere or pellet of frozen D-T mixture, for instance--is rapidly heated and promptly begins to fly apart on a very short time scale, τ, corresponding to the ratio of the pellet radius divided by the thermal speed of the ions $(2kT/M)^{1/2}$. While strictly this represents an unconfined system there is a small but non-zero time in which the plasma density remains adequately large. For a pellet size suitable for electricity generation, this time is about 50 psec and one must arrange conditions to achieve enough nuclear interactions in that time to produce useful amounts of energy. The "confinement" time can be increased somewhat by inclusion of tampers of higher density material to lengthen the time of disassembly.

Like its gravitational counterpart, inertial confinement fusion is known to work--in the form of the hydrogen bomb--thus, again, on an unacceptable scale. A major thrust of inertial confinement fusion research, therefore, is to show that very small amounts of D-T can be used successfully. For reference, the complete burning of one milligram of D-T will produce about 350 MJ; thus a reactor scenario based on inertial fusion might call for 10 microexplosions, each

burning 1 mg of D-T, to take place in a reactor vessel every second. If the output energy of the reactions (3.5 GJ per second) is absorbed in a thermal blanket, then--allowing for the inefficiency of converting the heat to electricity--one arrives at an electrical power output of ≈ 1 GWe. Also for reference, 1 MJ is roughly the energy released when half a pound of TNT explodes.

A magnetically confined plasma can be heated successfully by beams of neutral deuterium atoms or by radio-frequency waves or, perhaps, by beams of heavier atoms such as carbon. For inertially confined plasmas, energy supplied in the surface layers of a pellet by laser light or short-range ions causes ablative implosion of the pellet and can result in satisfactory compressional heating. It will be seen later (1.2) that volume compression of the fuel is in any case required for other reasons.

1.2 The Lawson Criterion for Magnetic and Inertial Confinement

While the condition for the product, $n\tau$, is roughly the same for magnetic and inertial fusion, the individual values of n and of τ needed are dramatically different for the two cases. A simple version of the criterion for ideal energy breakeven follows straightforwardly from energetics. If the number densities for deuterium ions and tritium ions are each denoted by n (thus total number density = 2 n) then the reaction rate is

$$R = n^2 \overline{\sigma v} \quad cm^{-3}sec^{-1} \qquad 1.$$

where $\overline{\sigma v}$ is the product of the interaction cross-section times the ion thermal velocity averaged over a Maxwellian velocity distribution. Figure 1 shows that $\overline{\sigma v}$ for the D-T reaction at 20 keV is about 4×10^{-16} $cm^3 sec^{-1}$. If the fusion reactions were to proceed for a time τ (short compared with the depletion time), then:

$$\frac{\text{Energy out}}{\text{Energy in}} = \frac{n^2 \overline{\sigma v} \tau (17.6 \text{ MeV})}{2n (20 \text{ keV})}$$

$$\approx 2 \times 10^{-13} n\tau \qquad 2.$$

giving a minimum scientific breakeven condition of $n\tau \gtrsim 5 \times 10^{12}$ $cm^{-3} sec$.

A more practical interpretation of $n\tau$ is as a measure of the fraction, ϕ, of the heated fuel that is burned in a time τ. At any time the rate of depletion of one fuel component (either D or T) is $-dn(t)/dt = \overline{\sigma v} [n(t)]^2$. Integrating for a time, τ, and setting $\phi = 1 - n(\tau)/n$, we find, for a temperature of 20 keV,

$$\frac{\phi}{1-\phi} = \overline{\sigma v} n\tau = 4 \times 10^{-16} n\tau \qquad 3.$$

In some early experiments on magnetic fusion with pulsed fields, τ was controlled by the pulse length of the equipment. Today, however, experiments are planned with fields maintained for times of the order of a minute; in that case the important time scale is the "energy confinement time" of the plasma, which is determined by the rate of escape of energetic particles and radiation from the hot plasma. This time can be of the order of a second so that at densities of $n \sim 10^{15}$ cm^{-3} a significant fraction of the fuel can be burned.

For $\phi \approx 30$ percent fractional burn, an $n\tau$ product of 10^{15} $cm^{-3}sec$ is needed.

Equations (1-3) also apply, of course, to inertial fusion with some additional constraints. The confinement time, τ, before the pellet has disassembled by virtue of the thermal speed, v, of the ions, is of the order of (r/v) where r is the radius of the fuel pellet. (More exact calculation indicates that the effective τ is close to one-quarter of this value.) To define an individual scale for either n or τ requires a further constraint. If we choose to specify explicitly the pellet mass, M, one can write

$$n\tau = \frac{M}{(m_D + m_T)} \cdot \frac{3}{4\pi r^3} \cdot \frac{r}{v} \gtrsim 10^{15} \text{ cm}^{-3}\text{sec}$$

or

$$\frac{M}{r^2} \gtrsim 7 \text{ g cm}^{-2} \qquad 4.$$

where the ion speed has been taken to be 2×10^8 cm/sec appropriate to 20 keV. Thus for a pellet of mass $M = 1$ mg, which is in the range of interest for inertial fusion, the fuel radius must be no more than 0.1 mm. This in turn implies, with $n\tau = 10^{15}$, that the number density n should be 2×10^{25} cm^{-3} or about 1000 times the density in solid D-T. Thus successful burning of an inertial fusion pellet requires that a sphere of solid-density D-T be compressed a factor of 10 in radius; the corresponding tenfold decrease in confinement time, τ, is more than offset by the thousand-fold increase in density, n. (From Equation 4, we note that had we chosen a larger value for M less compression would be needed, but the energy yield would become unacceptably large.)

Compression of the fuel by one-thousand fold, needed in any case to meet the Lawson criterion for milligram masses, brings with it an important side benefit. At normal DT solid density ($\rho = 0.2$ g cm^{-3}), the reaction product α-particles have a range of about 10 mm--ten times the pellet radius--and escape. Since the range varies as $1/n$, in the compressed fuel it will be 0.01 mm or about one-tenth of the compressed pellet radius. Thus most of the α-particles will stop in the fuel and help to raise its temperature. Under these "ignition" conditions not all the fuel needs to be heated to 20 keV ab initio; it is enough to compress the fuel and adequately heat a small central core whereupon the α-particles will take up the role of heating the surrounding fuel layers, thereby creating a "propagating thermonuclear burn wave."

Among workers in the inertial fusion field the Lawson criterion is usually stated in different units, viz. density, ρ in g cm^{-3}, and compressed fuel radius, r in cm. These quantities are directly proportional respectively to n and τ (a temperature of $\sim$ 20 keV being implicit); a more exact calculation than that used above shows that in these terms:

$$\phi = \frac{\rho r}{\rho r + 6}, \qquad 5.$$

so that a typical rule of thumb for significant fuel-burning is:

$$\rho r \gtrsim 3 \text{ g cm}^{-2} \qquad 6.$$

1.3 Inertial Fusion: Advantages and Issues

Magnetic fusion had already been a subject of substantial experimental study by the time the field emerged from beneath the umbrella of classification in 1956. Now it has reached the point where adequately high temperature and adequate confinement have been separately demonstrated in two different tokamak experiments and we are on the threshold of a further experiment (TFTR) in which both conditions are expected to be achieved simultaneously and scientific breakeven established. After the physics is proved will come the time to address the formidable engineering problems of making a realistic reactor system. The first wall, the thermal blanket (and breeder blanket, if there is one) must be incorporated close to the plasma within the complicated magnetic confinement coil system, and has to be designed so that it can be serviced and maintained after it has become radioactive. The complicated topology of toroidal, as opposed to mirror, devices makes this especially difficult.

The history of controlled inertial fusion is younger than that of magnetic fusion by some ten years and it is probably fair to say that, today, there continues to be a lag in the level of physics understanding of about five years or so behind magnetic fusion. It was shortly after Maiman demonstrated a practical working laser in 1960 that it was realized by Nuckolls et al (reported by Emmett et al 1974) that such a tool might provide the enormously high surface-heating power needed to compress and burn small volumes of thermonuclear fuel (Nuckolls et al., 1972). Declassification of

certain ideas that supported "laser-fusion" as an approach to electrical power generation took place early in the 1970's although design details and procedures for certain types of pellet continue to be classified. Using a neodymium-glass laser, Basov (1968) observed the first thermonuclear neutrons from a laser-heated plasma. Later, when it was found that particle beams (electrons and, later, ions) could offer special advantages as high-power drivers the name "laser fusion" was broadened to "inertial confinement fusion" (ICF) or "inertial fusion," for short.

While some years must elapse before the physics issues in inertial confinement can be settled, it could offer practical advantages over magnetic fusion for energy applications. In particular, the reactor vessel, which contains the microexplosions and converts their energy to heat, can be designed with a great degree of freedom with very few constraints imposed by the design of the driver which supplies the energy to the pellet surface. There is more choice, such as in the nature of the reactor materials or the size and shape of the vessel, than for magnetic systems, and the absence of the high magnetic field allows liquid metals to be used to protect the inner surface of the reactor. Design for maintenance is also eased. A second advantage is the appreciation--following the initial suggestion by Maschke (1974, 1975a)--that, not alone would an intense beam of high-energy heavy ions provide a particularly effective way of imploding pellets, but that we could capitalize on several decades of ideas and developments in the accelerator field to shorten the tedious engineering steps between scientific breakeven and a working

power-plant (Martin 1975, Martin and Arnold 1976, Keefe 1976). Realization of these advantages, however, requires certain physics questions to be resolved for the pellet, and the extrapolation of the accelerator physics from present practice to be shown.

The central issue for the pellet physics is whether a small amount of D-T fuel can be burned successfully under laboratory conditions. While a thermonuclear weapon is known to work, it releases a gigantic amount of energy and requires a high power driver--a fission device--also of colossal magnitude. It is impossible to extrapolate with certainty any of this experience to the scale of one-milligram pellets. A major issue for the small pellet is whether the large compression can be accomplished in a hydrodynamically stable way and the fuel heated in a delicately prescribed way; if, for instance, premature heating ("pre-heat") occurs, the fuel mass cannot be compressed enough and will fizzle. The Shiva laser at Livermore has succeeded in achieving volume compression to 50-100 times solid density, albeit with a very small mass and hence with a ρr value orders of magnitude below what is needed (Equation 6). A major issue for the driver--even if it be a single-shot device to test the pellet physics--is the ability to couple energy from the beam to the surface layers of the pellet; as will be seen later, laser and particle beams have quite different properties. Finally, for fusion power generation it is essential that the driver have high repetition rate (1-10 Hz), high efficiency (10-30 percent or more), high availability (> 80 percent), i.e. long-term reliability, and long lifetime.

2 PELLET COMPRESSION

2.1 Target Design Considerations

To this point the term "pellet" has been used in a simplified sense to denote a tiny sphere of D-T, but as will be seen here the configuration of the fuel and its attendant structure is more complicated. Hence the term "target" to denote the object placed at the focus of the laser or particle beams will be used from here on.

Figure 2 illustrates two classes of target design, the so-called "single-shell" and "double-shell" concepts. The outside layer of material in each consists of an ablation layer; when energy from laser light or short-range ions is deposited there, material is ejected and, just as in a rocket engine, an inward force is created by virtue of the outward momentum of the ablated material. In the single-shell design the fuel layer consists of a hollow shell of D-T--which can be created by filling the sphere with high-pressure gas and then freezing it. The object is to maintain a smooth, stable, ablatively-driven implosion until the fuel eventually ends up at the center with an appropriate ρr value close to 3 g cm^{-2}. From a simple one-dimensional rocket equation it is easy to estimate that for an energy-efficient implosion some 80 to 90 percent of the mass of the ablator will finally be ejected. If the compression occurs under ideal conditions, it turns out that, while the compressional heating of the fuel can be quite modest (on average ~ 200 eV), a small volume in the center can be raised to ~ 20 keV by the converging shock-wave

created in the fuel. This is exactly the desired condition for ignition to occur at the center and a burn-wave due to α-particle heating to propagate into the rest of the fuel. The double-shell design differs in having a small mass of D-T fuel contained in a shell of dense material suspended at the center. In this case the outer shell is driven inwards for a while, collides and transfers energy to the inner shell and drives the inner fuel to ignition. The burn wave then progagates outwards to the main fuel layer and ignites it.

Successful compression is a delicate operation, and it is essential to minimize the energy into the fuel until compression is complete. Direct transfer of energy from the ablator layer can be prevented by a pre-heat shield (see Figure 2). In addition, however, the implosion speed must be controlled rather carefully so that the compression is isentropic, in which case the pressure-volume variation is described by an adiabatic curve, or adiabat; for minimum heating the compression must take place along the lowest possible adiabat. Ideally, for maximum compression, one wishes to approach a condition where the electrons are in the Fermi-degenerate state in which case the average fuel temperature can be as little as ~ 200 eV for a ρr value of 3 g cm^{-2}. If premature heating of the fuel occurs it will begin to expand before a suitable value of ρr can be reached; alternatively, a very large driving energy would be needed.

Considerable attention is paid by target designers to minimizing the bad effects of fluid instabilities such as the Rayleigh-Taylor instability. This occurs whenever one attempts to accelerate a light

fluid against a dense fluid. For example, the buoyancy force of water cannot support a denser liquid above its surface; the interface is unstable and the liquids will begin to interchange. Similar instabilities can occur initially as hot low-density ablating plasma pushes cold high density material inward and again, later, just before the end of compression when the compressed hot fuel begins to exert an outward force against heavier material. In the double-shell design this instability can occur at both the outer and the inner shells. While the occurrence of fluid instabilities cannot be avoided, it is possible by proper choice of materials and geometry to ensure that the characteristic growth time can be adequately long to avoid effects that could be too damaging.

For the case where the input energy is derived from a beam of heavy-ions an alternative to ablative implosion has been proposed by Bangerter and Meeker (1976). Unlike laser light, high-speed heavy ions deposit most of their energy near the end of their range (Bragg peak). Furthermore, specific energy deposition is about twice as great in low-Z materials than in high-Z materials. Figure 3 shows a target design that takes advantage of these properties. Most of the ion energy is deposited in a subsurface layer of polyethylene (CH_2) which is seeded with a very small amount of tantalum oxide to inhibit preheat of the fuel. The thin outside layer of lead acts as a relatively immobile tamper that retards the outward motion of the expanding plasma. The action can be compared to that of a cannon--the gun-barrel containing the explosion--as opposed to the rocket-like action of ablatively driven targets.

Finally, the discussion of the target physics in this paper is treated entirely in the context of spherically symmetric illumination. In fact, that is not necessary and target designs are possible for which the energy is supplied by just two beams (or two bundles of beams) impinging 180 degrees apart. (From a practical point of view, two-sided illumination from opposite poles is much easier to arrange for in a reactor scenario than is spherical illumination.) In this case, one possibility is to convert the focused energy of the laser or particle beams to soft x-rays which, if contained in a black-body cavity ("hohlraum"), can provide spherically symmetric compression of a physically separate component containing the thermonuclear fuel. While such indirectly-driven target designs lie beyond the scope of this paper, the same sort of physics issues discussed herein are also involved.

2.2 Energy and Power Needed for Successful Compression

Results of elaborate computer programs (such as LASNEX at Lawrence Livermore National Laboratory) show that the desired implosion velocity should be close to 2×10^7 cm sec^{-1}. To achieve this the material in the ablator must be raised to a temperature of some 200 eV which, in turn, will require a specific energy deposition, w, in the ablator of

$$w \approx 20 \text{ MJ g}^{-1} \qquad 7.$$

This is one of three fundamental requirements that a laser or particle-beam driver must be able to provide.

A second requirement arises from the total amount of energy that must be supplied to the DT fuel. Ignoring the relatively small amount of energy needed to ignite the center portion and assuming the average fuel temperature can be kept as low as 200 eV one finds that the heat energy in a milligram is about 10 kJ. About an order of magnitude more energy must be supplied to the ablator, however, since the ejected ions carry away most of the energy and at best only some can be transferred to the remaining part of the ablator, or "payload," in rocket terminology. Thus the driver must be called upon to supply at least 100 kJ in energy. More realistic evaluation of several other effects such as fluid instabilities, imperfections in target fabrication, or illumination asymmetries, all of which affect ignition and burning, leads to about another order of magnitude in the driver energy, Q, requirement. Thus:

$$Q \approx 1 \text{ MJ} \qquad 8.$$

A third requirement arises through the short-time scale of the compression process. If, for instance, the targets in Figure 2 were initially 3 mm in radius they would be compressed to 0.3 mm in radius in a time of $0.27/(2 \times 10^7)$ sec $\approx$ 14 nsec. From the previous requirement (Equation 8) it is clear that the power, P, needed is given by

$$P = 1 \text{ MJ} / 14 \text{ nsec} \approx 7 \times 10^{13} \text{W} = 70 \text{ TW}$$

A more relevant quantity is the power per square centimeter, or irradiance, S, which for this example can be seen to be of order

10^{14} W cm^{-2}. Another argument to establish the order of magnitude of the power density required arises from the fact that the ablator surface layers are extremely hot (~ 200 eV) so that if one wishes to avoid significant cooling due to black-body radiation, an irradiance $S \approx \sigma T^4$ is needed, where σ is the Stefan-Boltzmann constant, 5.67×10^{-12} W cm^{-2} deg^{-4}; this, too, demands that $S \gtrsim 10^{14}$ W cm^{-2}. This argument, while helpful in setting a general scale, is in practice not strictly applicable; the plasma layer, in fact, is optically thin and the radiation loss will be well below the black-body level. In summary, careful considerations lead to the condition--probably the most demanding of all:

$$S \approx 2 \times 10^{14} \text{ W cm}^{-2} = 200 \text{ TW cm}^{-2} , \qquad 9.$$

Finally, successful target compression, i.e. maintaining the fuel conditions on a low adiabat, requires that the supplied energy pulse be shaped in time rising from a low power value at first to the peak value for the last 10 nsec or so. The performance of single-shell targets is somewhat more sensitive to maintenance of the proper pulse-shape than that of double-shell targets.

3 APPLICATION OF INERTIAL FUSION TO ELECTRIC POWER PRODUCTION

3.1 Target and Driver Requirements

Figure 4 summarizes the results of computer calculations of target gain versus input driver energy, gain being defined as the ratio of the energy arising from the micro-explosion to the energy supplied to the target by the driver (Coleman et al 1981a). It is clear that double-shell targets can achieve higher gains than single-shell targets when a sufficiently large driver energy is available ($\gtrsim$5 MJ). The rapid decrease in the double-shell gain curve as one proceeds downwards in input energy below 3 MJ seems an inevitable consequence of the two-step nature of that design.

What value of target gain may be needed for electric power production is intimately connected with the properties of the driver as can be seen by reference to a simplified power-flow diagram (Figure 5). The driver efficiency, η, is defined as the energy per pulse delivered by the laser or particle beam to the target divided by the total electric energy required to produce that pulse. Of the gross electric power produced, an amount fP is recirculated to operate the driver and the remaining amount, $(1-f)P$, represents the net generating capacity of the system. If the thermoelectrical conversion efficiency of the turbine generators is denoted by ε ($\approx$ 33 percent), the total power can be written

$$P = \eta(fP)\, G\varepsilon \qquad 10.$$

where G is the target gain. If one demands for economic and other reasons that the recirculating-power fraction be fairly small ($f = 1$ corresponds to no net power) then

$$1 >> f = \frac{1}{\eta G \epsilon} \approx \frac{3}{\eta G} ,$$

or, for example:

$$\eta G \gtrsim 10 . \qquad 11.$$

Thus the efficiency of a proposed driver system plays a crucial role in determining the target gain needed. Reference to Figure 4 shows that to achieve an ηG product of 10 a driver with 5 percent efficiency (characteristic of a good laser system) requires a double-shell target to achieve gain $G = 200$ and an input energy per pulse of 7 MJ. If the driver efficiency is as much as 25 percent (characteristic of a particle beam accelerator) the situation is greatly eased; the minimum gain needed is $G = 40$, which permits either single- or double-shell targets to be used, and the beam energy can be as low as 3 MJ per pulse. Because they are easier to make and cost less, single-shell targets are to be preferred.

To achieve significant amounts of electric power requires several microexplosions per second inside a containment vessel (reactor). Although the repetition rate needed is less for the higher gain targets, the impulsive wall-loading per event will be an order of magnitude larger for the example just given, namely $(200 \times 7)/(40 \times 3) \approx 12$ times.

While the energy release per pulse in the high-gain case corresponds to that from several hundred pounds of TNT the nature of

the explosion is, however, quite different from a chemical detonation. Most of the energy is carried to the walls by neutrons, x-rays and ions. Since the effect of a blast wave varies directly as the square-root of mass, for a given energy, the small target mass results in a shock to the wall some two orders of magnitude less than that due to a chemical explosion. Nonetheless, the more rapid succession of smaller explosions appropriate to a high-efficiency driver makes it easier to ensure that the containment vessel can be kept to a reasonable size (radius $\approx$ 5-10 m).

Table II summarizes the requirements that a driver for an electric generating system must fulfill.

Historically, lasers have provided the major tools for studies of the target physics problems in inertial fusion largely because they could supply the enormous irradiance that is needed. As candidates for a power-plant driver, however, they seem unpromising. Solid-state lasers (e.g. neodymium-glass) have low efficiency (< 1 percent), and thermal cooldown requirements restrict them to single-pulse operation. Gas lasers offer the possibility of the needed repetition rate since the active medium can be circulated and cooled. The carbon-dioxide laser may have too long a wavelength (10 μm) to be satisfactory for the conventional targets discussed here although its efficiency can approach 10 percent. Certain lasers that use excimers such as krypton fluoride have the advantage of suitable wavelength (0.25 μm) but would require heroic optical systems and are limited in efficiency to about 5 percent. The major problem facing the laser as a power-plant driver, however, is one that has emerged only in the

past couple of years, namely, that operation with double-shell targets will demand an energy per pulse approaching 10 MJ unless target gains can approach the ideal curves. This is 500 times the energy of the SHIVA glass laser at Livermore and 100 times that of the NOVA glass laser now under construction (Coleman et al. 1981b) and would cost far too much.

Light ion systems based on pulsed power technology, and heavy ion systems based on high energy and nuclear physics accelerator technology, share the advantages of experience with multi-megajoule beams and can have electrical efficiencies in the region of 25 percent, perhaps more. Production of intense light ion beams is, however, still a single-pulse operation; also, achieving the proper irradiance may require an unacceptably short distance between the accelerator and target (< 1 m). High-energy accelerator systems that can produce heavy ion beams have a wide theory and technology base and have demonstrated high repetition rate and availability. While the high beam-power needed in a heavy-ion beam of good optical quality appears theoretically feasible, it lies far beyond present experience and needs some scaled laboratory demonstration to ensure success.

Other methods that have been suggested for imploding targets include macroparticle acceleration, free-electron lasers, and imploding liners, but all these methods seem conceptually relatively less mature.

3.2 Reactor Considerations

Studies of the likely costs of fusion power plants employing either magnetic or inertial confinement have generally shown that the unit cost of the electrical energy produced decreases as the size of the plant is increased. This result, labelled "economy of scale," leads to the choice of an output capacity of 1 GWe--give or take a factor of two--as suitable for electricity production at a cost per kilowatt-hour comparable to that of today. (Who knows what may still be an acceptable cost fifty years in the future?) An additional design criterion derived from cost studies is that the wall of the fusion reactor should be able to operate at a high neutron loading in excess of 1 MW m^{-2}, preferably two to four times that value; the problem of wall survival at such levels is treated below.

A plant to produce 1 GWe requires a thermal input power of some 4 GWt (if one assumes a recirculating-power fraction, f = 25 percent) which can be generated by some 5 or 10 microexplosions per second each with a yield of 800 MJ or 400 MJ. Suitable targets would thus contain just a few milligrams of DT fuel. A suitable reactor design should

1. for single pulses: provide adequate containment, handle the conversion of the energy in the neutrons, x-rays, and target debris to a thermal blanket and, also, breed enough tritium to make up at least for what has been consumed;
2. for multiple pulse operation at 5-10 Hz: be restored to steady state conditions in about 100 msec and, also, have a target injection system with a 5-10 Hz capability.

Recently, Monsler et al (1981) have reviewed in comprehensive fashion the problems envisioned in reactor design and the possible solutions.

3.2.1 SINGLE-PULSE REQUIREMENTS About 70 percent of the energy released from the burning target is in the form of neutrons, distributed in energy with a peak at 14.1 MeV, and a degraded spectrum at lower energies because some neutrons interact before they can escape from the target debris. The remaining 30 percent of the energy is delivered mainly by x-rays and some by the hot ionized target debris. During the brief time (< 0.1 ns) when thermonuclear interactions are at their peak a significant amount of energy is emitted as hard x-rays with energies of about 100 keV. Shortly thereafter, the target debris that has been heated by absorption of α-particles, neutrons, and x-rays radiates soft x-rays in the 1 keV energy region. As this hot plasma debris expands and cools, the radiation spectrum shifts downwards in wavelength to optical and thermal emission. Note that the neutrons and hard x-rays will distribute their energy volumetrically, i.e., deep in the thermal blanket material, but because they arrive promptly they cause a thermal shock and thermal gradients which the structure must withstand. While the soft x-rays and debris arrive on a somewhat longer time-scale, their energy is deposited in a shallow surface layer on the inside of the wall and may produce significant erosion by evaporation and sputtering.

The thermal transients in the bulk material are amenable to conventional engineering design but wall erosion presents a special

concern in a chamber of reasonable size (no more than 10 m in radius) which is under vacuum. Stainless steel, for example, would be eroded at a rate of several centimeters per year. If required, engineering realizations of the "dry-wall" concept are possible by use of expensive materials, such as pyrolitic graphite or niobium, or by means of a sacrificial liner that could be replaced every few years (Hovingh 1976).

In an effort to arrive at a design for a containment vessel that could last for the life of a power plant (30 yr) several schemes for providing wall-protection have been devised. One of these, SOLASE, calls for the use of a buffer gas, e.g. neon or xenon, that is relatively opaque both to x-rays and to the debris ions (Conn et al., 1977). If the gas pressure is held at several Torr, the burning fuel rapidly creates around it a sphere of hot ionized buffer gas. This "fireball" expands until it cools to the point where its characteristic radiation can no longer be transmitted through the surrounding gas. At the point where the fireball expansion slows down, however, an outward-going shockwave is launched, propagates through the buffer gas and delivers a severe mechanical shock to the chamber wall, creating additional structural difficulties. The SOLASE concept is not applicable for particle beam drivers which require quite different gas pressure regimes for propagation but could be used for a laser driver, the buffer gas being transparent at optical frequencies.

Alternative ways of protecting the chamber wall to achieve a 30-year life rely on liquid metals, and several variants of this

concept have been proposed. In one early version, HYLIFE (Maniscalco, 1977), a curtain, or "fall," of liquid lithium is constructed inside the chamber wall. If the curtain thickness is chosen to be 60 cm the neutrons will deliver some 95 percent of their energy to the lithium while it will absorb essentially all of the x-ray and debris energy. Thus the heat energy can be removed by passing the liquid lithium through the primary of a heat-exchanger ahead of the turbines and then returning it to the top of the chamber to continue to supply the fall.

Apart from providing wall protection and allowing for rapid heat extraction from the chamber the use of liquid lithium fulfills the other condition mentioned earlier for single pulse operation, namely the breeding of tritium. The breeding ratio, defined as the amount of tritium bred per pulse divided by the amount consumed by thermonuclear burning, clearly should be unity or a little greater for a reactor that is self-sufficient in tritium supply. Two isotopes of lithium are efficient for breeding tritium by the reactions $^{7}Li(n, n'\alpha)T - 2.46$ MeV, and $^{6}Li(n,\alpha)T + 4.8$ MeV, the first reaction being due to fast neutrons and the second to slow neutrons. Neutronics calculations have shown that there is no difficulty in obtaining a tritium breeding ratio of between one and two. By breeding enough to supply the tritium needs of the targets, the tritium inventory at a power plant can be kept relatively low (several kilograms) and radiation hazards due to accidental tritium release minimized. Because the tritium is bred, it is interesting to note that the raw materials that are actually consumed are deuterium and lithium both of which, fortunately, are abundant.

A valuable byproduct of a fast-flowing liquid sheet of lithium in the chamber is that operation at high vacuum is possible. The vapor pressure of lithium at a temperature of $660^{o}K$--a desirable temperature for reactor operation--is about 10^{-4} Torr, which is low enough to allow propagation of the beams from a heavy-ion driver from the wall to the target. Lower pressure, if desired, can be arranged by operating at a slightly reduced temperature; for instance, at $610^{o}K$ the vapor pressure is 10^{-5} Torr. If the liquid lithium flows at a fast enough rate it also serves as a high-speed vacuum pump to restore rapidly the high-vacuum condition between pulses.

There are other candidates for a low-vapor pressure fall besides lithium but the need for breeding cannot be ignored. A suitable choice is a lead-lithium alloy Pb_4Li which would allow a lower lithium inventory (Maniscalco 1977). The lead degrades the neutron energy spectrum but a breeding ratio of unity can be maintained by a modest enrichment with ^{6}Li. A penalty for the use of this denser material results from the greatly increased pumping capacity needed to recirculate the liquid.

While a big step forward in ensuring long reactor lifetime, the continuous liquid metal fall does not eliminate some problems due to impulsive mechanical shock on the wall. At this low pressure, there is no fireball occurrence but the combination of evaporated material from the fall and the high central temperature leads to a rapid expansion that drives the fall rapidly and coherently outwards to slam into the chamber wall. A variation of the HYLIFE concept that overcomes this defect replaces the continuous curtain by a forest of

some 400 high-speed cylindrical jets, each about 5-15 cm in radius (Monsler et al 1979). The hot expanding gases can find a variety of tortuous paths among the cylindrical jets and the force is primarily taken up in liquid-liquid impact of the colliding jets. The jets are visualized to be arranged in a close-packed hexagonal array, to provide maximum screening of the wall, with a few lines of sight through the forest to allow the laser or ion beams to penetrate freely to the target. Finally, an alternative way of protection by an array of liquid-metal columns is discussed in a recent study for a heavy-ion driven fusion plant by a Karlsruhe - University of Wisconsin collaboration (Badger et al. 1981). Here the high-speed lithium jets are replaced by low-speed streams of lead-lithium alloy guided vertically by flexible tubes made of loosely-woven silicon carbide fibers. The main liquid flow is within the tubes but enough seeps through the weave to provide a substantial protective layer on the outside. Because this concept, called INPORT, seems to offer solutions, not just for single-pulse wall protection, but also for the many additional problems associated with repetitive pulsing at several hertz, it is discussed in the next section.

3.2.2 REPETITIVE-PULSE REQUIREMENTS Operation at 5-10 Hz demands that conditions inside the containment chamber be restored to normal within 100-200 msec. (This is not a hard and fast criterion since one can appeal to a design with a small number of separate stacked vessels into which the driver beams can be sequentially switched on successive pulses and the allowed restoration time thereby extended.) In the

SOLASE concept, for example, a large amount of heat is generated in the buffer gas and the thermal transfer to the vessel is so slow that it must be pumped out and replaced by cold gas between pulses (Bohachevsky 1981). In the HYLIFE concept the disrupted jets must be given time to reassemble into their steady state. As a result, repetition rates more than about 2 to 4 Hz will be difficult and require high pumping speeds for the liquid metal.

The INPORT concept circumvents many of the foregoing problems, provides a solution for operation at 5 Hz, and offers some additional advantages (Figure 6). By conducting the bulk flow of the lead-lithium alloy through woven SiC tubes the time delay associated with reassembly of a free-flowing jet is avoided. Also the fact that the conducted flow can hence be at a slow rate avoids the need for a comparatively massive pumping system, an early argument against the use of heavy liquid metals. The seepage of material through the coarse weave provides a protective layer of about 1 mm that is quickly evaporated by the x-rays and target debris but is reestablished on a time scale of ~ 100 msec. The lead-lithium alloy has a much lower vapor-pressure than lithium and even a working temperature as high as $500^{o}C$ still allows an operating pressure less than 10^{-5} Torr, comfortably low for the propagation of heavy-ion beams to the target.

In a pure lithium liquid metal system two concerns are, first, the chemical fire hazard due to the large hot lithium inventory and, second, the delicate operation of recovering the tritium from the hot lithium. Both are significantly ameliorated if lead-lithium alloy is used. The amount of lithium is reduced by more than an order of

magnitude. Also, tritium has a low solubility in lead-lithium alloy and will predominantly remain behind in gaseous form in the chamber, and thus it can be pumped out and recovered cold by cryogenic pumping systems.

A Westinghouse study (Sucov et al 1981) on a dry-wall concept that used an unprotected tantalum first wall contained the novel suggestion that advantages could be gained by having chemical overlap between the materials used in the target fabrication and those used in the containment vessel. They suggested, for example, that the high-Z tamper be made of tantalum rather than lead. Thus the deposition of material from the target debris could offset the erosion of the tantalum first wall. An analogous approach is advocated in the HIBALL study in which the lead tamper is retained but the pusher material, described in Section 2.1 as polyethylene seeded with tantalum oxide, is replaced by lithium seeded with a small fraction of lead with the same average density. Since this provides a quite acceptable target design one can thereby avoid the need to remove unwanted target debris from the liquid-metal coolant.

Finally, a working reactor requires the delivery of five, or more, cryogenic targets per second to the center of the chamber and overall system feedback to ensure that the target arrival and the driver pulse occur simultaneously. In a vessel of radius 10 m the time for free fall under gravity exceeds a second, hence the target must be launched at high velocity. Also it is desirable to delay target injection until the chamber conditions have been restored to steady state. Several satisfactory schemes for target injection, for

example, by electrostatic, electromagnetic or pneumatic means, are known and can impart speeds of the order of a few hundred meters per second which leads to a time for the target to travel the radius of the chamber of 50 msec or less. This time exceeds substantially the time interval between initiation of the driver pulse and arrival of the beams in the chamber so that the synchronization strategy consists in laser-ranging and tracking the ballistic motion of the target as it crosses the chamber, predicting its time of arrival at the beam focus, and firing the driver with a predetermined lead time. To take the specific example of a heavy-ion induction-linac driver (Section 5.2) the total travel time of the ions from rest at the ion source to arrival at the center of the chamber is about 100 μsec; thus, when the accelerator is first triggered, the target is only a couple of centimeters from the desired rendezvous at the center of the chamber. For proper operation of the accelerator the switching times of the accelerating modules need to be controlled to some 10 nsec; if this is characteristic of the timing error in the arrival of the beams it corresponds to a target positional error of only a few microns--negligible compared to the target size. While the longitudinal synchronization is not a problem, correction measures may be needed for lateral displacements, i.e. when the pellet trajectory does not intersect the center of the chamber. The input beam lines therefore must incorporate deflecting elements--movable mirrors for laser light beams or pulsed magnets for particle beams--that can be actuated in response to the target tracking information. Fortunately, the needed steering corrections are small, less than 1 mrad in angle, and pose no serious problems.

4 LASER DRIVERS FOR INERTIAL FUSION

4.1 Laser Interaction with Matter

This is an immense subject (Brueckner and Jorna 1974, Motz 1979, Bodner 1981, Max 1981) and can only be dealt with here in a summary and qualitative way. Some recent results of relevance to inertial fusion will be given in later sections. It should be noted that many early experiments in laser fusion made use of small glass microballoons filled with a D-T gas mixture to produce thermonuclear neutrons. In this case the thin shell is heated all the way through and explodes inwards and outwards to produce a rather small compression and a high-temperature fuel. Experiments with these "exploding-pusher" microballoons have little relevance to the sort of inertial fusion target conditions discussed above, where it was seen that an intact ablatively-driven shell must produce large volume compression and, at the same time, maintain the fuel conditions on a low adiabat.

In considering the laser as a candidate for an inertial-fusion driver one must examine two basic issues: (a) Coupling Efficiency, and (b) Hot Electron Production. The "coupling efficiency," defined as the ratio of the energy usefully conveyed to the DT fuel divided by the input energy in the laser light, is made up of two factors, the "implosion efficiency" and the "absorption efficiency." The implosion (or hydrodynamical) efficiency enters in the consideration of any kind of driver and represents the effectiveness of the ablatively-driven rocket action in conveying maximum energy, first, to the imploding

pusher shell or payload and, second, in conversion of this energy into convergent non-adiabatic shock-heating of the fuel. The question of fluid instabilities in the target is also common to all drivers. The absorption efficiency, however, which measures how well the incoming radiation is converted to mass-ablation of the pusher, depends very much on the nature of the driver. For instance, heavy ions are believed to deposit their energy in well-understood classical fashion and not to create penetrating hot electrons. Laser light, on the other hand, must contend with a multitude of complicated physical processes that occur in the corona region that extends out beyond the ablation surface, and the absorption efficiency is an especially sensitive function of many parameters associated with the laser pulse, e.g. wavelength, irradiance, pulse length, etc. The second issue, hot electron production, can prove fatal if it leads to excessive preheating of the fuel; it also turns out to be critically dependent on the laser light parameters.

Several large research programs in the U.S. and elsewhere are addressed to unravelling the variety of physical processes at play and determining how they scale. While present lasers provide more than adequate irradiance, they fall short by two orders of magnitude in the energy needed for reactor-sized targets (millimeters) and, hence, must conduct experiments on scaled down sizes and for short pulses. Development of accurate scaling laws that can be extrapolated with confidence is, therefore, of the highest priority. Figure 7 is a schematic of coronal conditions. To first order, absorption of the light occurs predominantly in that part of the corona where the plasma

density has the critical value, n_c ($\sim 10^{21}$ cm^{-3} for $\lambda = 1$ μm), such that the plasma frequency, $\omega = (4\pi n_c e^2/m_e)^{1/2}$, matches the angular frequency of the laser light. Light energy is absorbed basically by three mechanisms: (a) Inverse bremsstrahlung, (b) Resonance absorption, and (c) Parametric instabilities.

In the first process, electrons oscillating in the electric field of the light wave collide and exchange energy with the ions. (Its title derives from the change in the energy state of both an electron and an ion following absorption of a photon.) At low laser intensities this collisional process dominates by far and is a desirable one in that only low temperature electrons are generated. As one proceeds to higher intensities, collective plasma processes begin to predominate, for example the second and third ones above, both collisionless, in which the incoming electromagnetic wave is coupled to a variety of plasma waves through both linear and non-linear processes. The high electric fields produced by such waves can have the undesirable result of generating hot electrons (>> 20 keV) and, consequently, penetrating x-rays also. It should be noted that partition of energy among these absorption mechanisms is also a function of wavelength, in particular the collisional loss being enhanced as one proceeds to shorter wavelength.

Not all the laser light energy is absorbed, however, and as one proceeds to high intensity an increasing fraction is lost by reflection through stimulated Brillouin and stimulated Raman back-scattering. (Again, these effects are relatively weaker at short wavelengths.) The nomenclature arises by analogy with light

scattering from sound waves (Brillouin) or from molecular vibrations (Raman); the corresponding waves in the corona are the ion acoustic oscillations and electron plasma oscillations, respectively, which are pumped, or stimulated, by the laser light. Both Brillouin and Raman scatter represent instability processes in that the scattering contributes energy to the corresponding plasma wave. As a result they can also generate hot electrons. Raman scatter leads to an absolute (i.e. restricted to one location in space) instability at the point where the coronal density is $n_c/4$. Both effects also can lead to convective instabilities which drift away from the region of interaction; if such instabilities are growing, their total growth depends on the scale-length of the plasma. As mentioned earlier, limitations in total energy allow laser experiments at appropriately high power only for short times and small sizes and the magnitudes of the effects remain uncertain for scale lengths and times appropriate for reactor targets. Theoretical estimates for millimeter scale plasmas place the fraction of light reflected by Brillouin back-scatter between 30 percent to 90 percent, a disturbingly wide range (Bodner 1981).

The mechanism of thermal conduction which translates the energy absorbed at the critical layer into the ablation front is not yet properly understood and remains a topic of intensive study. On the one hand, the energy flow may be inhibited and can result in loss of efficiency. On the other hand, however, thermal diffusion effects can be large and can serve to smooth out the consequences of local hot spots at the critical layer and provide more uniform energy transfer

to the ablation face, thus allowing considerable departure from symmetry in the driving beams.

4.2 Laser Facilities and Experiments

4.2.1 AVAILABLE WAVELENGTHS The primary tools in use today for studies of laser fusion are the neodymium-glass laser ("short" wavelength, λ = 1.06 μm) and the carbon dioxide gas laser ("long" wavelength, λ = 10.6 μm). In addition, in anticipation of the advantages of operating at very short wavelengths, development of krypton-fluoride gas lasers (λ = 0.25 μm) is actively underway. One of the most dramatic advances in the last few years has been the demonstration that laser light at higher harmonics (e.g. $\lambda/2$, $\lambda/3$, $\lambda/4$) can be efficiently generated, thus greatly extending the range of experiments on the critical issue of wavelength scaling of the many physical processes occurring in the corona. Most of the Nd-glass facilities have now been modified to include this capability, and experiments have recently been made not just with infrared light (λ = 1.06 μm) but also with green ($\lambda/2$ = 0.53 μm), blue ($\lambda/3$ = 0.35 μm) and even ultraviolet ($\lambda/4$ = 0.26 μm) light. Frequency conversion can be achieved by passing the red light through an optically non-linear medium, such as a potassium dihydrogen phosphate (KDP) crystal. The polarization density in the crystal responds to the incoming light like an anharmonic oscillator and develops components at the harmonics $\lambda/2$, $\lambda/3$, etc., which can be radiated. High conversion efficiency ($\approx$ 70 percent) has been shown for $\lambda/2$ and $\lambda/3$ light (Coleman et al 1981c).

4.2.2 SHORT WAVELENGTH LASERS Major inertial fusion programs based on glass lasers are conducted at Lawrence Livermore National Laboratory (LLNL), KMS Fusion, Naval Research Laboratory (NRL), and the University of Rochester (UR) in the United States and also at Ecole Polytechnique (France), Osaka (Japan), Rutherford-Appleton laboratory (United Kingdom) and the Lebedev Institute (USSR). The largest program and facilities are at LLNL, where recent experiments have been done with the two-beam Argus system (2 kJ, 5 TW) and the twenty-beam Shiva system (10 kJ, 20 TW). See Figure 8. Both of these facilities have now ceased operation as preparations for installation of a much larger system, Nova, are proceeding. It will be constructed in two stages, Novette with two beams, and Nova with 10 beams. Each beam will have the capability of providing 10-15 kJ and 5-15 TW. Novette is scheduled to be completed late in 1982 with the larger system following within a few years. The accomplishments at Shiva include the ablatively-driven compression of fuel to 100 times liquid density and the successful implosion of double-shell targets.

The 24-beam system, Omega (4 kJ, 12 Tw), at UR, has begun operations and is an upgrade of their previous 6-beam system, Zeta. The KMS system (1 kJ, 2 TW) incorporates a unique gas-jet target system to allow experiments on absorption and stimulated Brillouin scatter under conditions of various density-gradients. Most of the above systems have some measure of frequency-conversion capability and have contributed greatly to the experimental study of wavelength-scaling. A key result is the way the energy absorption efficiency falls off with intensity at different wavelengths.

Figure 9 shows clearly the advantage of the shorter wavelength where the absorption mechanism at high irradiance is dominated by inverse bremsstrahlung. Figure 10 shows another important result, the sharp drop-off in hot electron production, inferred from the x-ray spectra, as the wavelength is decreased; it can be seen that a factor of three reduction in wavelength from 1.06 μm reduces the penetrating x-ray flux by more than two orders of magnitude and results in a more favorable, i.e. steeper, slope in the spectrum.

Experiments at NRL have concentrated on detailed studies of ablative acceleration of planar targets by relatively long laser pulses (3 nsec). Although the laser energy and power are comparatively low (1 kJ, 0.3 TW), they have been successful in achieving ablation-driven velocities of 10^7 cm sec^{-1} with both high absorption and hydrodynamic efficiencies, and with only small heating of the rear surface (relevant for preheating effects). It still remains an issue how these results are to be scaled to the higher power needed for fusion targets.

While Nd-glass lasers continue to provide a valuable research tool for studying the physics of laser light interactions and certain features of fuel compression, it should be noted that they are quite unsuited as a driver for an inertial fusion power plant. After a single high-power pulse the glass must be allowed to cool down and return to thermal equilibrium, which requires a time of about one hour for the largest systems built. Steady operation at many pulses per second is inconceivable. Also, the electrical efficiency is about 0.1 percent, two orders of magnitude below the region of interest for fusion power.

4.2.3 LONG WAVELENGTH LASERS Carbon dioxide lasers (λ = 10.6 μm) offer a number of practical advantages. The efficiency can be relatively high, as laser systems go, perhaps approaching $\eta \approx 10$ percent. Also, the use of gas as an active medium allows the engineering design of a driver with high repetition rate since the gas can be recirculated and cooled on a continuous basis.

Studies with carbon-dioxide lasers are centered at the Los Alamos National Laboratory. The two-beam Gemini system operated--until its recent shut-down--at 1 kJ and 1 TW, and the larger eight-beam Helios system delivers 8 kJ at 8 TW. Under construction, at present, is a still larger system, Antares, which will have 24 beams and deliver 40 kJ at 40 TW; it will be completed in 1983 (see Figure 11). Experiments at Helios have achieved fuel compression to 20 times liquid density in small targets.

The major issue, however, is whether the physics of absorption and hot electron production, at this long wavelength, can in fact allow successful ablative implosion and ignition of reactor targets. Much has been made earlier of the apparent benefits of proceeding to wavelengths shorter than 1.06 μm, and an obvious question arises as to how much less favorable the physics may be for a wavelength ten times longer. The answer seems to point to the need for developing radically different target designs and, indeed, some new concepts have been proposed that could turn to advantage the physics observed for 10.6 μm light.

Experiments on hot electron production at different irradiances at wavelengths from 0.26 μm up to 10.6 μm are consistent with a

scaling law that gives a mean electron temperature proportional to $(S\lambda^2)^k$, where $k \approx 0.33 - 0.46$. This behavior is inferred from measurements of x-ray and ion fluxes and is therefore dependent on details of the theoretical modelling--hence the uncertainty in the exponent, k. The penetrating electrons generated by CO_2 light are, therefore, five to ten times hotter than those produced by Nd-glass light, for the same irradiance. Priedhorsky et al (1981) report observing a hard x-ray spectrum with a slope of 250 keV at $S = 10^{16}$ W cm^{-2} in an experiment at the Helios facility. They also claim that a substantial fraction, probably between 10 percent and 100 percent, of the absorbed laser energy is converted to hot electrons.

Thus the target designer is immediately presented with two challenges: how to avoid preheat without the use of an intolerably massive preheat shield, and how to convert the energy of the electrons into a more useful form. In response, several new concepts have been developed. One interesting possible solution has been proposed by Lee et al (1979) in the form of "vacuum insulation." Normally, the inward flux of hot electrons from the coronal region generates an outward return current (to maintain charge neutrality) carried by the cold plasma electrons. If a vacuum layer is introduced behind the outer foil shell (engineering details like maintenance of the vacuum and mechanical support are ignored) the return current is eliminated and the emission of a small number of hot electrons will make the outer layer positively charged and any further electron emission is inhibited by the electric field (Figure 12). Indeed, electrons that

start inwards can be returned to reflex backwards and forwards through the outward shell to deposit their energy as useful heat. The envisaged action is similar to that in a reflex ion diode (see Section 5.1). Eventually, however, ions will be emitted from the inner surface of the outer foil and move across the vacuum gap to give electrical closure. The net effect is to change the time-scale from that appropriate for fast electrons to a slow ion time-scale. It is not clear, however, whether such a protection scheme can be scaled to reactor-sized targets.

The long wavelength light has been found, also, to lead to substantial fluxes of ions with MeV energies from the coronal region. In seeking to explain many experimental observations of thermal transport inhibition, Forslund and Brackbill (1981) have made a major advance in the understanding of not just thermal transport but also the fast ion production. When laser light is focused to a spot on a thin foil a density gradient occurs in the direction of the light and a thermal gradient predominantly in the transverse direction towards the spot. Under these circumstances azimuthal magnetic fields in the megagauss range can occur, their strength and rate of rise being greater the hotter the electron temperature. Hot electrons emitted backwards from the front surface are trapped by the magnetic field (cf magnetic insulation discussed in Section 5.1) and spread transversely across the foil surface far away from the focal spot by a fast $\underset{\sim}{E} \times \underset{\sim}{B}$ drift motion. This has three important consequences: (a) the energy of the electrons is held trapped in the coronal region, (b) the energy deposited at the focal spot is rapidly convected sideways to provide

thermal smoothing over a large area, and (c) the thin sheet of electrons hovering just above the foil surface results in the formation of an ion diode (cf Section 5.1) which extracts ions from the surface plasma and accelerates them back towards the incoming laser light. Because of their higher magnetic rididity, the ions can cross the shallow region of magnetic field without being trapped.

Ions of several MeV kinetic energy pose no threat of pre-heat because of their short range and indeed, as discussed later, provide a much more desirable energy deposition mechanism than do fast electrons. In the example calculation by Forslund and Brackbill (1981) about 20 percent of the total absorbed energy was converted to ions. This suggests the intriguing possibility of finding suitable conditions such that most of the absorbed energy can be transferred from the electrons to fast ions; preliminary experimental results are very encouraging.

While this may seem, at first sight, an unnecessarily complicated way of heating by light ions compared with a directly-accelerated light-ion beam, it circumvents the major problem of propagating a high-current light-ion beam several meters across the reactor (Section 5.1) by using the laser light as an intermediate vehicle to place the ion source within a millimeter, or so, outside the target.

4.2.4 ADVANCED LASER DEVELOPMENT Lasers that use gas as an optical medium offer the potential for operation at high repetition rate. Given the recent promising results on absorption efficiency and hot-electron spectra as one proceeds to shorter wavelength, it is not surprising that the krypton-fluoride laser (λ = 0.25 μm) has become

the object of attention as a fusion driver. Practically it can reach an efficiency of about 5 percent. Difficulties still remain with developing optical coatings to handle the power densities in the ultraviolet region in a reasonable way. A discussion of the strategies and laser architecture options can be found in a recent comprehensive review by Holzrichter et al (1982).

5 PARTICLE BEAM DRIVERS FOR INERTIAL FUSION

In many aspects charged particle beam drivers represent the antithesis of laser systems. We have seen that laser systems suffer from relatively low efficiency, will be costly to scale to the many-megajoule energy range needed, and have many unanswered questions about absorption efficiency and preheat. Nonetheless, lasers provide a unique way of developing the huge irradiance required because the power can be delivered to a tiny focal spot. Particle beam drivers, on the other hand, include a variety of accelerator technologies that can have high electrical efficiency (25 percent and more), have demonstrated multi-megajoule capability, and are believed to deposit energy in a classical and well understood manner without significant problems of preheat (with the exception of electron beams). In contrast with lasers, the major issues concern reaching adequately high beam power on a small focal spot, 2 or 3 mm in radius. In particular, heavy ion drivers stand unique in being based on technology developed over many years for accelerators for high energy and nuclear physics and so can guarantee high repetition rate, long life and high availability.

Both particle-beam and laser drivers must meet the needs described earlier set by the target performance (see Table 2). For practical reasons, however, the higher electrical efficiency of accelerators permits the use of single-shell targets so that the beam energy per pulse in a fusion power plant can be less than that for lasers by a factor of two or more. The whole class of problems

associated with the corona is absent. (In a sense, particle beams represent the ultimate in a short wavelength system having de Broglie wavelengths in the range 10^{-6} - 10^{-11} μm!)

As discussed in Section 2.2, successful implosion of a target demands an irradiance $S \sim 2 \times 10^{14}$ W cm^{-2}, a specific energy deposition $w \sim 20$ MJ g^{-1} and a time-scale $t \sim 10^{-8}$ sec. Since $w = St/R$, where R is the particle range in g cm^{-2}, one quickly notes that no matter what ion is used, its range is constrained to be close to $R = 0.1$ g cm^{-2}. This constraint has dramatically different consequences for the kinetic energy and current of the beam, depending on the mass of the ion; typical specifications are:

1. For electrons: ~ 1 MeV and 100 megamperes
2. For protons: ~ 5 MeV and 20 megamperes
3. For heavy ions ($A \gtrsim 200$): ~ 10 GeV and 10 kiloamperes.

5.1 Light Ion Drivers

This approach has its roots in a technology for producing intense relativistic electron beams (IREB) that was pioneered more than thirty years ago by C. Martin at Aldermaston, England. In its commonest form an IREB accelerator consists of a slowly pulsed high-voltage supply, such as a Marx generator, which charges a pulse-forming line to a few megavolts; this energy can be switched to a rather simple cold cathode diode in which the electron beam is generated either by field-emission or emission from a surface plasma (Nation 1979). Such a pulse-power system is relatively simple and inexpensive to fabricate. Typical

IREB currents lie in the range from 10 kA to several megamperes and the largest systems can deliver megajoules of beam energy in a pulse duration of some 100 nsec or less. This form of pulse power technology is useful basically for single-pulse operation and would require extensive modification to achieve high repetition rate. Nonetheless, in the near term it offers the advantage of operating at much higher beam energies (megajoules) than any existing laser system. For testing of target physics the biggest issue is whether beams can be focused to provide adequately high irradiance.

Early experiments were pursued with electron beams principally at Sandia National Laboratory, Albuquerque, and at the Kurchatov Institute, Moscow. Apart from the difficulty of focusing electron beams with such enormous current on a small spot, the electrons have an ill-defined range and also produce x-rays; hence preheat can be troublesome to avoid. The realization in the mid-1970's that IREB diodes could be converted to produce huge currents of light ions (protons) led to a dramatic switch in the Sandia program from electrons to ions in 1979. Already under construction at that time was a radial array of 36 separate electron-beam machines, each with its individual diode arranged so that the electron beams would converge at the center of the array. The voltage polarity was quickly reversed, the electron beam diode designs abandoned and replaced by a design for a single cylindrical ion diode to give an inward-pointing ion beam, and the name of the device changed from EBFA (electron beam fusion accelerator) to PBFA-I, the first letter now standing for "particle" (Figure 13). This system has operated electrically at

1 MJ, 30 TW into a dummy load. Experiments with ion diodes at another Sandia facility, Proto-I, have already achieved an irradiance of 2 Tw cm^{-2} on a target.

The brief history of the development of high-current ion diodes has indeed been explosive--proceeding from a few hundred amperes (Humphries et al 1974) to present values of 700,000 A (Cooperstein et al 1979). Also, about 80 percent of the electrical energy going into the diode can be converted to ion energy. The amazing variety of high-current ion-diode designs and their performance have been reviewed by Kuswa et al. (1982). The key to sucessful operation lies in the suppression of electron flow. In a conventional IREB diode, electrons emitted from the cold-cathode rapidly cross to the anode foil which thereupon quickly develops a surface plasma which produces ions that stream back towards the cathode. Under these conditions of bi-polar Child-Langmuir flow, the backward proton current density is 2.3 percent of the electron current density, down by the square-root of the mass-ratio. Thus almost all of the power of the generator goes to the electron beam and little to the ions. A wide variety of techniques has now been devised for inhibiting the electrons from crossing the gap, in which event efficient power transfer from generator to ions can be accomplished.

Three generic methods of electron suppression are shown in Figure 14; many hybrid designs have also been used (Kuswa et al. 1982). In the reflex diode (Figure 14a) electrons lose a small amount of energy in passing through the anode foil, fail to reach the second cathode and reflex backwards and forwards through the foil many times

with decreasing amplitude. Thus the electron current is severely reduced but the electrons, nonetheless, help provide charge neutralization for the ions by virtue of their presence. The reflexing electrons produce an anode plasma which is the source of the ions. Notice that half of the ions in the case depicted will be lost because they are directed unfavorably.

Figure 14b shows a schematic of the concept of magnetic insulation in which a transverse magnetic field causes the electrons to execute magnetron-type orbits, thus preventing them from crossing the gap. The simplified version shown would work only for a short time, since negative charge accumulation near the top of the cathode would soon lead to electrical breakdown. A wide variety of ingenious designs has been developed to arrange the magnetic field configuration to have cylindrical symmetry--either about the axis of a planar diode or by developing the diode into a cylindrical diode formed by two co-axial annuli to produce an inward-pointing sheet beam (barrel diode). In either case, the $\underset{\sim}{E} \times \underset{\sim}{B}$ drift carries the electrons around the symmetry axis many times and charge accumulation is avoided. In a magnetically-insulated diode the ions come from an anode surface plasma created by an electrical flashover; the cathode can be a thin foil or mesh to allow the ions to escape.

The usual text-book treatment of the Child-Langmuir space-charge limited current in a planar diode makes use of a one-dimensional model. This is adequate for many conventional applications in which the self-magnetic field of the beam is unimportant since the self-field cannot be incorporated in a one-dimensional model in which

the beam has no axis and no boundary. The pinched electron beam diode (Figure 14c) relies heavily on the self-magnetic field of the electrons to create mainly radial flow of the electrons (the more rigid ions will flow almost axially) and thus greatly prolong the electron transit time from cathode to anode. It is well known that an intense electron beam cannot propagate axially through a background of charge-neutralizing positive ions if the current exceeds the Alfvèn-Lawson limit, $I = 17{,}000\ \beta\gamma$ amperes, the value at which the self-field at the beam edge can bend an electron into an arc of diameter equal to the beam radius [$\beta = v/c$, $\gamma = (1 - \beta^2)^{-1/2}$]. The pinched-beam diode relies on the electron current being high enough that the self-magnetic bending radius of electrons near the beam edge is somewhat less than the anode-to-cathode gap spacing, d, and electrons flow (in complicated orbits) in the radial direction as sketched in Figure 14c. This will occur if the electron current leaving the cathode exceeds $I = 17{,}000\ \beta\gamma(r/2d)$ amperes, where r is the cathode radius, and lies beyond the Alfvèn-Lawson limit for the usual geometries where $r/2d > 1$. Although ion flow is mainly axial in the different ion diodes discussed, the ion currents can substantially exceed the Child-Langmuir value computed on the basis of the physical spacing of the anode-cathode gap. This arises simply because the effective diode spacing is really much smaller because of penetration of the electron-cloud (virtual cathode) into the gap space.

While the Sandia program has included many experiments on ablative implosion of cylindrical foils and successful production of high temperature (50 eV) imploded plasma, their major efforts are

directed at obtaining higher irradiances with the proper time-structure at PBFA-I, mainly by testing different diode designs and different methods of focusing and progagating the beams to the target (Yonas 1981). Recent efforts have been devoted to the use of the AMPFION (auto-magnetic, plasma-filled, ion-) diode (see Figure 15) In this, the electric current pulse from the generator into the diode is made to flow through spiral conductors arranged radially to produce an insulating magnetic field with a constant tangential magnetic field at the surface of the anode plasma. The design of the complicated conductor arrangement takes into account the self-field of the ion beam. This design has been found susceptible to damage by the huge particle fluxes, and is costly to fabricate or repair. Also, ions crossing the region of the insulating magnetic field receive small transverse magnetic deflections in various directions which smear out the energy-deposition region at the target and limit the irradiance. The possibility of proceeding to diode designs that could produce heavier ions, such as carbon, is therefore being examined. A promising prospect for the near future is the "pinch-reflex diode" developed at NRL and it will soon be tried at PBFA (Cooperstein et al 1979). This is a modification of the pinched beam diode (Figure 14c) in which the electrons are caused to reflex through a thin anode foil. The geometry is arranged to produce a convergent (ballistically-focused) ion beam at 1.3 MeV which has been propagated through a plasma to produce current densities as high as 200-300 kA/cm^2 at the focal spot.

Construction of a new facility, PBFA-II, has begun at Sandia, and it should operate in 1986. Like PBFA-I, it will consist of 36 generators arranged radially but each with a higher power capability (3 TW) and a range of voltage options (2-16 MeV). With a total power in excess of 100 TW it is hoped to achieve an irradiance at the target of 50 TW cm^{-2}, which could be enough for breakeven. Just as in the case of PBFA-I, where the advantages of proceeding up the ion mass-scale (from electrons to protons) was perceived in the early design stages, plans for PBFA-II now incorporate the possibility of using still heavier ions such as helium, lithium, or carbon.

The research program at the Kurchatov Institute continues to center on the use of electron beams. Construction of a large 50-module radial array of generators, Angara 5, has encountered some technical difficulties and is proceeding slowly (L. I. Rudakov 1981, unpublished). As yet, there has been no indication of any intention or desire to convert the equipment to exploit the more promising ion diode approach.

5.2 Heavy Ion Drivers

5.2.1 ADVANTAGES, PARAMETERS AND ISSUES Figure 16 shows the range-energy relation for different ions in hot (200 eV) matter and illustrates the origin of interest in the use of accelerated heavy ions i.e. $A \gtrsim 200$. The values of range are not very different from those in condensed matter except for very short ranges below the level of interest. It can be seen that for the desired range in the pusher

of 0.1 - 0.2 g cm^{-2}, the energy of a ^{207}Pb ion (~ 10 GeV) is about one-thousand times greater than that of a proton (~ 10 MeV). Hence, to meet the irradiance requirement, the beam-current can be reduced from 20 MA of protons to 20 kA of heavy ions. While this is still a very large ion current, it has opened the possibility of using conventional accelerator technology that employs vacuum transport of beams by magnetic (or electric) lenses through multiple accelerating gaps. At high currents such as this, the beam plasma frequency $\omega = (4\pi ne^2/m)^{1/2}$ is large enough to result in significant corrections to conventional accelerator physics formulae; the physics of non-neutral plasmas, fortunately, is considerably different, and simpler to predict, than that of conventional neutral plasmas. It will be seen that the major physics issues reduce to the following two questions: (a) Can conventional accelerator technology be reliably scaled to produce 10 kA of ion current? (b) If so, can collective or other effects such as those due to non-linearities, be controlled well enough to ensure that the beam quality (brightness) is adequately good to allow it to be focused ten meters away on a spot a few millimeters across? Our present understanding of accelerator physics leads us to believe that both questions can be answered affirmatively for, in fact, more than one type of accelerator system. The design, however, must incorporate some special features: for instance, a beam current in the 20 kA range would require intolerably high magnetic fields for single channel transport and must be transported near the target in 10 or 20 separately focused channels.

Another feature of the reduction in particle beam current to 20 kA is the high degree of confidence one can have that the energy deposition in the target is describable in classical terms. Good theoretical arguments exist (Bangerter 1979) but, also, the experimental observation of classical energy deposition for protons at 1 Tw cm^{-2}--a particle fluence greater than that needed for heavy ions--provides a further basis of reassurance.

Using the information in Table II one can develop the list of parameters for a heavy ion accelerator driver given in Table III. For a target gain of G = 100, the energy release per pulse is 300 MJ, corresponding to burning 1 mg of DT fuel per pulse; at a repetition rate of 10 Hz, the electrical output is about 1 GWe.

The advantages of exploiting conventional accelerator technology are many:

1. There is a substantial physics and engineering base of experience, particularly in the fields of high energy and nuclear physics where it stretches back for 50 years. The wide repertoire of accelerator tools, concepts and devices that has been developed and tested, can be deployed with a high degree of confidence to meet this new challenge. Techniques developed for rapid beam switching and splitting or combining beams are highly applicable. There is some relevant experience with multimegajoule beams at Fermilab and CERN; while these are beams of relativistic protons and far from the 100 TW class, there is now considerable experience in such matters as the handling,

shaving, aborting and shielding of beams with this substantial damage potential.

2. Designs that incorporate high repetition rate, high availability and long lifetime have become commonplace in the conventional accelerator field. In the future development of inertial fusion on the road to a full-scale reactor, the proven feature of high-repetition rate is especially crucial. The engineering evaluation of a variety of containment vessel designs demands this ability to bring the vessel up to full temperature under realistic conditions for long test periods. All other proposed driver systems will require many years of difficult engineering to achieve this capability and, indeed, in some cases it may not be achievable.

3. As stressed earlier, high driver efficiency is extremely desirable for economic reasons and also in permitting the use of simpler low-gain targets with relatively low yield per pulse. Hitherto, the design of research accelerators has paid no attention to striving for high efficiency, although some accelerators (SLAC, LAMPF) do operate with an efficiency of several percent. Most designs for a fusion driver accelerator have naturally focused on accelerating as much beam current as possible so that, automatically, the higher beam loading has led to increased electrical efficiency from the mains to the beam. Typical estimates of accelerator driver efficiency lie in the range 20-30 percent; higher values seem possible at the expense of increased capital cost but would have a diminishing effect on the economics of fusion power.

5.2.2 ACCELERATOR PERFORMANCE CRITERIA The realism of proposed driver schemes has been the subject of extensive review by accelerator scientists at a series of workshops (Bangerter et al 1976, Smith 1977, Arnold 1979, Herrmannsfeldt 1980). At the time of the first workshop, target designers believed that an ion kinetic energy of 40-100 GeV and a beam energy as low as 1 MJ might be suitable; since then, the desired kinetic energy has dropped dramatically and the beam energy increased (see Table III). Both changes aggravate the accelerator problems significantly in requiring higher beam currents and causing greater difficulty in achieving a small focal spot. The central problem lies in achieving the high beam power which, as discovered by Maschke (1975b), is limited in a magnetic quadrupole systsem by practical field strengths; he showed that the transportable beam power scales as $(\gamma-1)(\beta\gamma)^{5/3}$ (see below) and thus is a steep function of ion kinetic energy. This limit comes into play when the electrostatic self-repulsion of the beam particles (magnetic self-attraction being almost absent at the speeds under consideration) becomes comparable with the magnetic restoring force of the transport lenses.

Another casualty of the changed target parameter specifications has been the synchrotron as a candidate for a driver system. The great attraction of the synchrotron as a tool for high energy particle physics lies in its ability to amplify proton energies by a factor of one thousand, or so, between injection and extraction. A heavy-ion synchrotron, for several reasons, needs a high injection energy (about 2 GeV at the Berkeley Bevalac, for instance) and, as the gap between the injection energy and the desired extraction energy dwindled to

only a small factor, its advantages were soon realized to be outweighed by the disadvantages of introducing the extra beam manipulations involved (e.g. injection, extraction, de- and re-bunching) and it was retired as a driver option (Teng et al 1979).

Nonetheless, two distinct accelerator system designs offer considerable promise of success (Teng 1976). One uses an rf linac patterned on conventional designs (Figure 17a) to accelerate about 100 mA of heavy ions to the full energy of 10 GeV. It differs from today's ion linacs in three regards, first, in the low charge-to-mass ratio of the ions ($q/A \approx .01$ compared with .1), second, in the high current ($I \gtrsim 100$ mA compared with $I \sim 5$ mA) and, third, in that several parallel injectors are needed to accelerate lower current beams at the front end--because of the velocity dependence of the Maschke limit--to an intermediate energy where they can be combined and safely transported thereafter (Figure 17a). This last operation requires careful manipulations in the transverse and longitudinal phase-planes to minimize emittance dilution and so preserve beam brightness. The main rf linac is a constant current device and simply serves to boost the kinetic energy to 10 GeV at a beam current of 150 mA. A three-stage system is then used to amplify the beam current by the required factor of 10^5. The beam is transferred to ten storage rings via an intermediate stacking ring and intermediate condenser rings to allow multi-turn stacking in both vertical and horizontal phase planes. By means of rf bunchers in the rings the current can be further increased and the pulse length shortened. Next the ten beams are simultaneously extracted from the storage rings,

each passed through a further pulsed bunching stage (provided by a ramped-voltage induction linac) and finally carried to the target.

The other scheme is a single-pass induction linac in which amplification of the beam-current takes place continuously during acceleration (Figure 17b). The induction linac consists of a sequence of non-resonant pulsed ferromagnetic cores, each of which supplies an energy increment to the beam by transformer action (Figure 18). This structure is particularly well suited to acceleration of very high beam currents, e.g. 100 - 100,000 A, in a repetitive pulsed fashion (Faltens and Keefe 1981). The ion injection current is several amperes (one hundred times that in the rf linac) and the entire beam can be accelerated in a single long sausage-like bunch. (Actually, there are cost advantages to subdividing the beam transversely and transporting several long bunches side by side in separate transport channels but all threading the same accelerating cores.) Early on, the voltage pulses to the induction cores are ramped slightly upwards with time, thus differentially accelerating the tail of the bunch with respect to the head. As the velocity is increased and the bunch length decreased, the beam current rises to several kiloamperes at the end of acceleration. A strongly ramped voltage is then applied to initiate a further longitudinal compression (by the needed last factor of 5 or so) which takes place in the final transport system to the target. An example of how the current and pulse length vary for a particular design is shown in Figure 17b. If a single beam were to be accelerated it must be split transversely by septum magnets and subdivided into 10-20 channels for transport to the target; obviously,

if acceleration of multiple beams (10-20 in number) were to be arranged, this septum-splitting operation could be avoided.

In choosing the detailed design parameters for either system, attention must be paid to several limiting phenomena arising from self-field (non-neutral plasma) effects at high current. Transverse effects limit the current, or lead to undesirable emittance growth; longitudinal effects lead either to beam loss or to an increase in momentum spread, $\Delta p/p$, with consequent chromatic aberration problems in the final focusing stage. When the beam plasma frequency is high, coupling can take place between these degrees of freedom and theoretical description of this coupling is still incomplete. Specific limitations that are known and must be considered in the design are as follows:

1. In the storage ring the Laslett (1963) tune-shift condition applies for transverse stability, i.e., the number, N, of stored ions is constrained by

$$N < \frac{2\pi\,\Delta\nu}{b r_p}\left(\frac{M}{M_p}\right)\left(\frac{1}{q^2}\right)\varepsilon_N \beta\gamma^2 \qquad 12$$

where b = bunching factor = (fraction of ring occupied by ions)$^{-1}$,

r_p = classical radius of proton = 1.5×10^{-16} cm,

q = ionization state of stored ions,

$\pi\varepsilon_N = \pi\varepsilon\beta\gamma$ = normalized transverse emittance

= constant in ideal accelerator.

For steady-state storage conditions the allowed betatron tune shift, $\Delta\nu$, has the value 0.25. In the final rapid bunching needed just before extraction, this can be exceeded for a transient situation; a bunching experiment by Maschke at the Brookhaven AGS showed that by rapidly passing through betatron resonances $\Delta\nu = 2$ could be attained. For a heavy ion driver $\beta(\approx 0.3)$, $\gamma(\approx 1)$, and $\varepsilon_N(\approx 2 \times 10^{-5}$ radian meters) are all small; thus the requirements set by Equation 12 demand that the number of storage rings must be large (10-20). Also, it is undesirable to use an ion with a charge state, q, much more than unity.

2. In the storage ring the longitudinal resistive instability can occur and consequently lead to an increase in momentum spread and loss of ions to the walls. This instability will not occur if the injected beam has a sufficiently large momentum spread. Unfortunately, a large momentum spread conflicts with the need to minimize chromatic aberration in the final focusing lenses, and it is found that in most driver scenarios the beam will always be above the instability threshold. Growth times will be of the order of a millisecond and damaging effects need not occur if injection, bunching, and extraction are all completed in a time of the order of a few milliseconds.

3. For linear beam transport systems the maximum current, and hence power, that can be transported in a quadrupole lattice is limited by the maximum attainable focusing (Maschke limit). This limit

has been the object of extensive analytical and numerical study (Smith 1981). The limiting beam power, P, in watts is given by

$$P = 1.7 \times 10^{15} \left(\frac{M}{qM_p}\right)^{4/3} \left(\epsilon_N B\right)^{2/3} \left(\beta\gamma\right)^{5/3} \left(\gamma-1\right) \qquad 13$$

where B = quadrupole "pole-tip" field (teslas) averaged along transport line.

Delivery of the needed power of 150 TW (Table III) to the target demands that some 10–20 beams must be used if this condition is to be obeyed.

Equation 13 can be rewritten as a limit on beam-current by dividing by the beam "voltage," $Mc^2(\gamma-1)/qe$, and in this form is an important design factor for an induction linac driver. An induction linac will be most compact and efficient if it is accelerating currents in the kiloampere range; the Maschke limit will not, however, permit such currents below a kinetic energy of some 2 GeV (Figure 17b) and the low-velocity section consequently must be less than ideally matched. A way of circumventing this current limit has, however, also been discussed by Maschke (1979) who pointed out that transverse subdivision into a number of beamlets each separately focused will allow more total current to be transported. A design for a four-beam induction linac has indeed shown significant cost advantages (Faltens et al 1981). As mentioned earlier, extension of this design to the range 10–20 beams would offer another benefit in avoiding septum splitting after acceleration.

4. The longitudinal resistive instability is not a problem for the rf linac (because the current is low) but must be considered in detail for the induction linac where the current is typically 10,000 times greater. Since one is dealing with a single bunch, the theory is incomplete. Simple theory suggests that two plasma waves are launched forwards and backwards from the site of a perturbation. The fast forward wave decays; the backward slow wave grows in amplitude as it travels to the back of the bunch but then is reflected into a forward-going decaying wave. Results from more sophisticated analyses give conflicting results, some predicting stability, others instability (Smith 1981). If instability does occur, the growth length λ is given by

$$\frac{1}{\lambda} = \frac{R}{Z_o}\left(\frac{4\pi^2 q^2}{1 + 2\ \ln(b/a)} \cdot \frac{M_p}{M} \cdot \frac{N}{L}\, r_p\right)^{1/2}$$

where R = Real part of impedance/meter,

b/a = Pipe radius / beam radius ≈ 1

Z_o = Free-space impedance = 377 ohms

N/L = line density of ions

Using a conservative value of R (100 ohms/meter), λ turns out to be of the order of one kilometer. In the length of a driver (5-10 km) growth may do little damage. Analysis of a type that indicated instability for a single-beam 3 MJ driver has shown that the situation becomes stable again by resorting to four parallel beams--an added benefit of the multiple-beam approach.

Since its inception in 1977, the heavy-ion fusion program in the U.S. has been seriously hampered by lack of funding and it has not yet been possible to test many of the key issues in the accelerator physics that must be explored before proceeding to build a large device. Nonetheless, experiments at Argonne, Brookhaven and Berkeley have been able to establish that heavy-ion sources with the needed high-current and high-brightness can be successfully built, also that the transport of very intense ion beams at low velocity can be handled successfully and conforms to theory. If a funding level comparable with that of the light-ion program (still much below that for the laser programs) is established it is planned to build an ion accelerator with an energy, 2-5 kJ, that will produce plasma temperatures of ~ 50 eV in a small focal spot. Such a test device would settle many of the accelerator questions, establish the predicted nature of ion energy deposition in hot matter, and also illuminate the problems that could be encountered in propagating intense ion beams in a reactor environment (Bangerter 1981). Based on today's knowledge the heavy-ion approach seems clearly to offer the most promising driver for a civilian power plant. The lack of proper financial support can be traced partly to its late entry into the field, and partly to the fact that the laser and light-ion approaches are primarily directed at the physics of scientific feasibility and weapons-related physics for which neither efficiency nor repetition rate is a concern.

5.3 Focusing of Ion Beams on the Target

This topic has been the subject of a recent intensively-referenced review by Olson (1982) in which he classifies the various methods that have been proposed for final focusing of the beams on the target as follows:

1. Ballistic transport with bare beam: Here the ions move in straight lines converging from the final lens to the target.
2. Ballistic transport with transversely-available electrons: In this case electrons are injected radially into the beam to supply neutralization of the self-repulsive space-charge force.
3. Ballistic transport with axially-available electrons: This differs from 2) only in the feature that the electrons are allowed to be dragged along the direction of motion of the ions.
4. Ballistic transport with co-moving electrons: If electrons can be injected at the same speed as the ions and in the same direction they can, ideally, provide perfect charge and current neutralization.
5. Ballistic transport in gas or plasma: If there is a background gas in the containment vessel it will rapidly be ionized by the incoming ions to provide some measure of neutralization.
6. Self-pinched transport in gas: If the ion beam can be focused to a spot size of a few millimeters and then passed through a gaseous region at a pressure of a few Torr, "self-pinched" propagation can occur. The background plasma produces charge neutralization and partial current neutralization; the net

current causes an azimuthal magnetic field to confine the beam to constant size within which the ions oscillate in the transverse direction.

7. Transport in pre-formed channel: Here a current-carrying conducting plasma channel is created ahead of time by means, for example, of a laser, an electron beam, or an exploding wire; the net current generates an azimuthal magnetic field that may confine the beam.

Two distinct sets of focusing issues must be faced for light ions. First, how does one achieve satisfactory focusing in the present generation of single-pulse experiments where the anode surface subtends a very large solid angle at the target, and the intrinsic spread in angles of the ions forces the stand-off distance from anode to target to be very short (~ 50 cm)? Second, how can one develop a focusing concept suitable for a reactor vessel where the propagation distance is of order 10 m, and the ports through which the ions enter must subtend a very small solid angle at the target?

For either light-ion application, the simplest focusing scheme in the list, (1), can be ruled out. For the near-term experiments with PBFA-I and -II, the focusing mechanisms, (2), (3) and (5), have received most attention; choice of proper anode curvature ensures the ions are launched on average to point directly at the target and are thereafter neutralized by electrons or plasma. It should be noted that the proton currents discussed lie near and above the Alfvèn-Lawson limit for protons, $I_A = 31\ \beta\gamma$ megamperes $\approx$ 3MA,

which implies that neutralization conditions must be maintained stably to a high degree of precision. Some two dozen plasma instability effects (e.g. two-stream, filamentation, etc.) have been examined theoretically and it is not yet clear whether one can stay out of danger from all at once. Also of concern is transient plasma behavior which may spoil the focusing during parts of the pulse. Some experiments at reduced power and energy have, however, provided encouragement for some approaches (Olson 1981). For a reactor scenario, only mechanisms (6) and (7) are options and the former can probably be ruled out insofar as the azimuthal magnetic fields generated seem too small to contain the beam. Some new instabilities, e.g. hose instabilities, arise in case (7) and are on the verge of being troublesome but probably are not fatal.

For heavy-ions all seven focusing mechanisms are candidates for consideration. The cleanest by far is the first, focusing in vacuum, and is amenable to precise classical calculation including treatment of high order aberrations (second and third) in the final magnetic quadrupole lenses. Provided the number of final beams is large enough (10-20) to maintain the current in each beam no greater than 1 kA, or so, a focal spot size of 2.5 mm radius can be achieved for low charge-state ions. Good vacuum ($< 10^{-4}$ Torr) is required but reactor concepts have been described that seem to have acceptable properties (Section 3.2). Almost all other options have been considered to some degree; if any were to succeed it could provide further flexibility in the choice of charge state (higher q), or a reduction in the number of final beams entering the reactor, or in

exploring a wider variety of reactor concepts. By contrast with light ions, the heavy ion current per beam entering the reactor is some six orders of magnitude below the ion Alfvèn-Lawson limit, $I_A = 6\ \beta\gamma$ gigamperes ≈ 2 GA, which eases the performance requirements of the various neutralization schemes. Whether there is a stable window of propagation in gas (5), or not, at a pressure $\sim$ 1 Torr, has been the subject of varied theoretical arguments; if it exists it may or may not be a wide enough window for reliable utility. Results of numerical simulation of injection of co-moving electrons (4) have been extremely encouraging in showing that some four times as much current per beamline as in the vacuum case can be acceptable; thus a smaller number of final beams, perhaps as few as four, might be permissible.

6 SUMMARY AND OUTLOOK

In future years, inertial confinement fusion can offer an inviting alternative to magnetic confinement fusion for electricity generation. In particular, a much wider variety of choice in the design of the reaction containment vessel is allowed since this method of confinement does not require the vessel to be cocooned within intricate field windings. Furthermore, the overlap between reactor design and driver design is minimal.

Whereas the development of magnetic fusion over the years has proceeded by trying to scale up the physics from small experiments to large ones, such as the Princeton TFTR or the Livermore MFTFB, the thrust of inertial fusion research is the opposite, namely trying to scale down the physics known to work for large uncontrolled devices to the tiny scale needed for controlled fusion. A critical issue is whether the physics will allow successful compression and burning of the fuel for a driver energy investment that is not too large--no more than several megajoules. If so, a second critical issue is development of a practicable driver in the megajoule class with high enough efficiency to make electricity economically. It is in this regard that particle-beam drivers offer the most promising solutions; also, they should achieve higher coupling efficiency than lasers because of the absence of coronal phenomena. The additional features of high repetition rate and ability to focus the beams at long stand-off distances make the heavy-ion approach, in particular, an attractive choice.

ACKNOWLEDGMENTS

I thank R. O. Bangerter, A. Faltens, T. Godlove, W. B. Herrmannsfeldt, R. Johnson, W. Kunkel and J. M. Peterson for reading early drafts and offering helpful comments and suggestions. My gratitude is due to S. E. Bodner, D. Breggink, T. Chan, W. F. Krupke, J. W-K. Mark, C. L. Olson, S. Rockwood and G. Yonas for providing graphical material. I especially thank Linda Egeberg for her patience and care in the preparation of the text.

This work was supported by the Assistant Secretary for Defense Programs, Office of Inertial Fusion, Laser Fusion Division, U.S. Department of Energy, under Contract No. DE-AC03-76SF00098.

Literature Cited

Arnold, R. C., ed. 1979. Proceedings of the Heavy Ion Fusion Workshop, Argonne National Laboratory, 1978. Argonne National Laboratory Report ANL-79-31. 430 pp.

Badger, B., Arendt, F., Becker, K., Beckert, K., Bock, R., Bohne, D., Bozsik, I., Brezina, J., Dalle Donne, M., El-Gueb-ly, L., Engelstad, R., Eyrich, W., Frohlick, R., Ghoniem, N., Goel, B., Hassanein, A., Henderson, D., Hobel, W., Hofmann, I., Hoyer, E., Keller, R., Kessler, G., Klein, A., Dreutz, R., Kulcinski, G., Larsen, E., Lee, K., Long, K., Lovell, E., Metzler, N., Meyer-ter-Vehn, J., von Mollendorff, U., Moritz, N., Moses, G., Muller, R., O'Brien, K., Peterson, R., Plute, K., Pong, L., Sanders, R., Sapp, J., Sawan, M., Schretzmann, K., Spindler, T., Sviatoslavsky, I., Symon, K., Sze, D., Tahir, N., Vogelsang, W., White, A., Witkowski, S., Wollnik, H. 1981. In HIBALL - A Conceptual Heavy Ion Beam Driven Fusion Reactor Study, pp. VI.1/1 - VI.7/12. University of Wisconsin Report UWFDM-450

Bangerter, R. O. 1979. See Arnold 1979, pp. 415-20.

Bangerter, R. O., compiler. 1981. Accelerator Fusion--A National Plan for the Development of Heavy-Ion Accelerators for Fusion Power, Los Alamos National Laboratory preprint LA-UR-81-3730, 32 pp.

Bangerter, R. O., Herrmannsfeldt, W. B., Judd, D. L., Smith, L., eds. 1976. ERDA Summer Study of Heavy Ions for Inertial Fusion, Lawrence Berkeley Laboratory Report LBL-5543. 110 pp.

Bangerter, R. O., Meeker, D. J. 1976. Lawrence Livermore Laboratory Report UCRL-78474. 15 pp.

Basov, N. G., Kriukov, P. G., Zakharov, S. D., Senatski, Yu. V., Tchekalin, S. V. 1968. IEEE J. Quant. El. QE4, pp. 864-67

Bodner, S. E. 1981. Journal of Fusion Energy 1:221-240

Bohachevsky, I. O. 1981. Los Alamos Scientific Laboratory Report LA-8557. 61 pp.

Brueckner, K. A., Jorna, S. 1974. Rev. Mod. Phys. 46:325-67

Coleman, L. W., Krupke, W. F., Strack, J. R., eds. 1981a. 1980 Laser Program Annual Report, Vol. 2, p. 3/18, Lawrence Livermore National Laboratory Report UCRL-50021-80

Coleman, L. W., Krupke, W. F., Strack, J. R., eds. 1981b. See Coleman et al 1981a, Vol. 1, pp. 2/53 - 2/183

Coleman, L. W., Krupke, W. F., Strack, J. R. 1981c. See Coleman et al 1981a, Vol. 1, pp. 2/254 - 2/286

Conn, R. W., Abdel-Khalik, S. I., Moses, G. A., Beranek, F., Cheng, E. T., Cooper, G. W., Droll, R. B., Henderson, T., Howard, J., Hunter, T. O., Larson, E. M., Kulcinski, G. L., Lovell, E. G., Magelssen, G. R., Maynard, C. W., Okula, K. R., Ortman, M., Ragheb, M. M. H., Rensel, W. B., Solomon, D., Spencer, R. L., Sviatoslavsky, I. N., Vogelsang, W. F., Watson, R. D., Wolfer, W. G. 1977. SOLASE, a Conceptual Laser Fusion Reactor Design, University of Wisconsin Report UWFDM-220

Cooperstein, G., Goldstein, S. A., Mosher, D., Oliphant, W. F., Sandel, F. L., Stephanakis, S. J., Young, F. C. 1979. Proc. 3rd Int. Top. Conf. on High Power Electron and Ion Beam Res. and Tech., Novosibrisk, USSR, 1979, pp. 567-75

Dean. S. O., ed. 1981. Prospects for Fusion Power, p. 3, Elmsford, N.Y.: Pergamon Press. 90 pp.

Emmett, J., Nuckolls, J., Wood, L. 1974. Scientific American 230(6):24-37

Faltens, A., Hoyer, E., Keefe, D. 1981. Proc. 4th Int. Top. Conf. on High-Power Electron and Ion Beam Res. and Techn., Palaiseau, 1981, ed. H. J. Doucet, J. M. Buzzi, pp. 751-758, Paris: Ecole Polytechnique. 996 pp.

Faltens, A., Keefe, D. 1982. Proc. 1981 Linear Accel. Conf., Santa Fe, N.M., Oct. 1981, pp. 205-13. Los Alamos National Laboratory Report LA-9234-C. 381 pp.

Forslund, D. W., Brackbill, J. U. 1981. Magnetic Field Induced Surface Transport on Laser Irradiated Foils, Los Alamos National Laboratory Report LA-UR-81-170. 12 pp.

Herrmannsfeldt, W. B., ed. 1980. Proceedings of the Heavy Ion Fusion Workshop, Berkeley, 1979, Lawrence Berkeley Laboratory Report LBL-10301. 515 pp.

Holzrichter, J. F., Eimerl, D., George, E. V., Trenholme, J. B., Simmons, W. W., Hunt, J. T. 1982. Journal of Fusion Energy. In press

Hovingh, J. 1976. See Bangerter et al 1976, pp. 41-44

Humphries, S., Lee, J. J., Sudan, R. N. 1974. Appl. Phys. Lett. 25:20-22

Keefe, D. 1976. Lawrence Berkeley Laboratory Internal Report BEV-3201. 7 pp.

Kuswa, G. W., Quintenz, J. P., Freeman, J. R., Chang, J. 1982. Chapter IV, Applied Charged Particle Optics, Part III, Advances in Electronics and Electron Physics, Supplement 13C, ed. A. Septier. New York: Academic Press. In press

Laslett, L. J. 1963. Proc. 1963 Summer Study on Stor. Rings, Accel., and Exp. at Super-high Energies, ed. J. W. Bittner, pp. 324-367. Brookhaven National Laboratory Report BNL 7534. 477 pp.

Lawson, J. D. 1957. Proc. Phys. Soc. (London), B, 70:2-10

Lee, K., Forslund, D. W., Kendel, J. M., Lindman, E. L. 1979. Nuclear Fusion 19:1447-56

Maniscalco, J. A. 1977. See Smith 1977, pp 73-75

Martin, R. L. 1975. IEEE Trans. Nuc. Sci. NS22:1763-64

Martin, R. L., Arnold, R. C. 1976. Argonne National Laboratory Internal Report RLM/RCA-1, and U.S. Patent 4,069,457

Maschke, A. W. 1974. Brookhaven National Laboratory Report BNL 19008. 6 pp.

Maschke, A. W. 1975a. IEEE Trans. Nuc. Sci. NS22:1825-27

Maschke, A. W. 1975b. Brookhaven National Laboratory Report BNL-20297. 3 pp.

Maschke, A. W. 1979. Brookhaven National Laboratory Report BNL-51029. 3 pp.

Max, C. E. 1981. Lawrence Livermore National Laboratory Report UCRL-53107. 82 pp.

Monsler, M., Blink, J., Hovingh, J., Meier, W., Walker, P. 1979. See Arnold 1979, pp. 225-236

Monsler, M. J., Hovingh, J., Cook, D. L., Frank, T. G., Moses, G. A. 1981. Nuclear Technology/Fusion 1:302-58

Motz, H. 1979. The Physics of Laser Fusion. London: Academic Press. 290 pp.

Nation, J. A. 1979. Particle Accelerators 10:1-30

Nuckolls, J., Wood, L., Thiessen, A., Zimmerman, G. 1972. Nature (London) 239:139-42

Olson, C. L. 1982. Journal of Fusion Energy 1(4):307-39

Priedhorsky, W., Lier, D., Day, R., Gerke, D. 1981. Phys. Rev. Lett. 47:1661-64

Smith, L. W., ed. 1977. Proceedings of the Heavy Ion Fusion Workshop, Brookhaven National Laboratory, 1977. Brookhaven National Laboratory Report BNL-50769. 146 pp.

Smith, L. 1982. Proc. 1981 Linear Accel. Conf., Santa Fe, N.M., Oct. 1981, pp. 111-115. Los Alamos National Laboratory Report LA-9234-C. 381 pp.

Sucov, E. W., ed. 1981. Inertial Confinement Fusion Central Station Electric Power Generating Plant, Vol. 1, pp. 4/75-6, Westinghouse Fusion Power Systems Report WFPS-TME-81-001. 234 pp.

Teng, L. C. 1976. See Bangerter et al 1976, pp. 13-17

Teng, L. C., Judd, D. L., Mills, F. E., Sutter D. F. 1979. See Arnold 1979, pp. 159-70

Yonas, G. 1981. Proc. Tenth Eur. Conf. on Cont. Fus. and Plas. Phys. (Moscow Sept. 1981). In press

FIGURE CAPTIONS

Figure 1 Values of $\overline{\sigma v}$ averaged over a Maxwellian distribution for a variety of fusion reactions.

Figure 2 Schematic cross sections of two types of target. The single-shell target (left) is simpler to fabricate. The double-shell target (right) has two regions containing D-T fuel, ignition occurring first in the inner one. The beam-deposition region may be a single layer of light or dense material or may be composed of several different layers.

Figure 3 A target designed specifically to be driven by ions. (left) Arrangement of tamper, pusher and fuel layers; (right) Energy deposition profile for 10 GeV heavy ions. Most is deposited in polyethylene seeded with tantalum oxide (TaCOH).

Figure 4 Calculated gain for single- and double-shell targets as a function of driver input energy (Coleman et al 1981a). Correction factors related to realistic experimental uncertainties reduce the gain estimates below those obtainable under ideal conditions (labeled "optimistic"). For double-shell targets, the gain drops rapidly for driver energies below the range plotted. The lines marked η = 5 percent, 25 percent, indicate the gain needed for drivers with these respective efficiencies (Equation 11).

Figure 5 Electrical power flow in a reactor. The recirculating power fraction is f.

Figure 6 The INPORT reactor concept (Badger et al 1981) which incorporates improvements over the HYLIFE concept (Maniscalco 1977). The coolant is a liquid lead-lithium alloy conducted in open-weave silicon carbide tubes. Ten ports through which the heavy ion beams enter are arranged in five pairs around the chamber; one pair is shown.

Figure 7 A schematic of the density and temperature distribution near the critical and ablation layers for a laser driver (Bodner 1981). Under ideal conditions the velocities of the payload and the ejecta are equal and opposite.

Figure 8 A view along the twenty-beam neodymium-glass laser system SHIVA.

Figure 9 Absorption efficiency for laser light as a function of irradiance, showing the advantage of using wavelengths less than 1 μm (corresponding to an angular frequency, ω_0) at high irradiance.

Figure 10 The x-ray spectra produced by hot electrons at $\lambda = 1.06$ μm and $\lambda = 0.35$ μm. Both the fluxes and mean energies decrease for shorter wavelengths.

Figure 11 One of the two carbon dioxide laser amplifiers for the 40 kJ, 40 TW Antares facility at Los Alamos. Each simultaneously amplifies twelve laser beams azimuthally arranged near the outer radius (see exit holes in end-plate at right). The medium is pumped by 48 high-current electron beams that emerge radially from the inner cylindrical chamber.

Figure 12 Experimental results of the effectiveness of vacuum insulation of the hot electrons (preheat signal). Measurements indicate even sharper cut-off than the calculated curve based on the model by Lee et al (1979).

Figure 13 A cut-away view of PBFA-I showing the arrangement of the Marx generators, pulse forming lines and transmission lines that lead to a cylindrical ion diode in a small region ($\approx$ 50 cm) at the center.

Figure 14 A schematic of the three general classes of ion diodes discussed (Olson 1982).

Figure 15 The AMPFION ion diode for use at PBFA-I (Kuswa et al 1982). The cylindrical symmetry is about a vertical axis. Current flowing to the diode through complicated spiral conductors provide magnetic insulation that traps electrons.

Figure 16 The range-energy relation for several ion species in hot matter (200 eV). The ion range of interest for inertial fusion is about 0.1 - 0.2 g cm^{-2}.

Figure 17 Schematic of two proposed accelerator driver systems: (a) the proposed 7 MJ driver for HIBALL of the rf/storage ring type first proposed by Maschke (Teng 1976). Current amplification occurs at full energy by multiturn stacking in a cascade of rings; a final factor of ten comes from induction bunchers; (b) a single-pass four-beam induction linac (3 MJ) in which current amplification occurs continuously to keep pace with the space-charge limit.

Figure 18 A view of the FXR induction linac at the Lawrence Livermore National Laboratory. In accelerates 4 kA of electrons with a pulse width of 60 nsec; components towards the high-energy end of an ion-induction linac would look very similar.

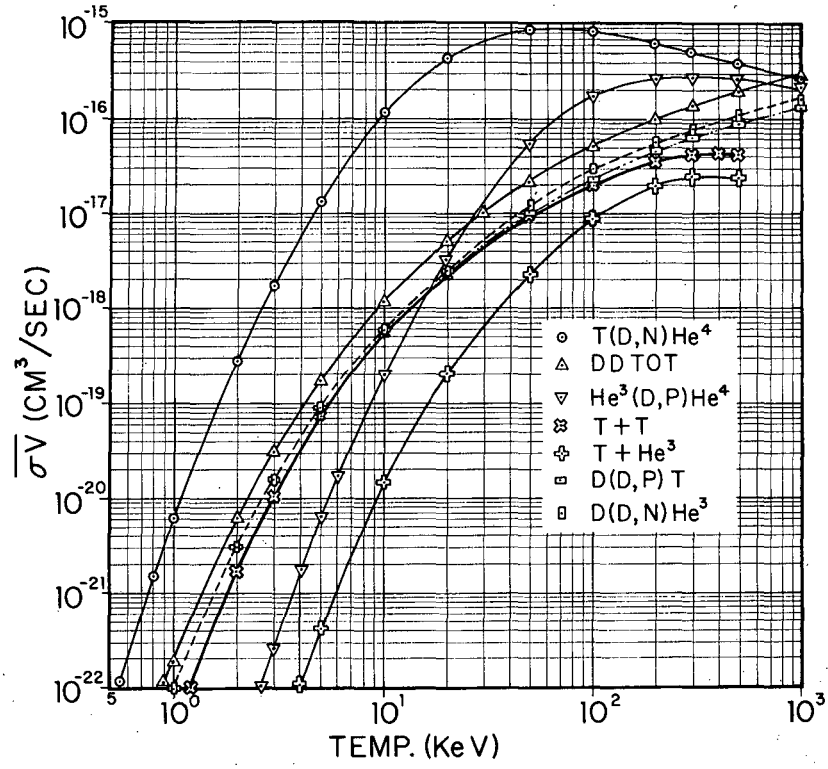
10^{-15}
10^{-16}
10^{-17}
10^{-18}
10^{-19}
10^{-20}
10^{-21}
10^{-22}
$\overline{\sigma V}$ (CM^3/SEC)
10^0
10^1
10^2
10^3
TEMP. (Ke V)
T(D,N)He^4
DD TOT
He^3(D,P)He^4
T + T
T + He^3
D(D,P) T
D(D,N) He^3

Figure 1

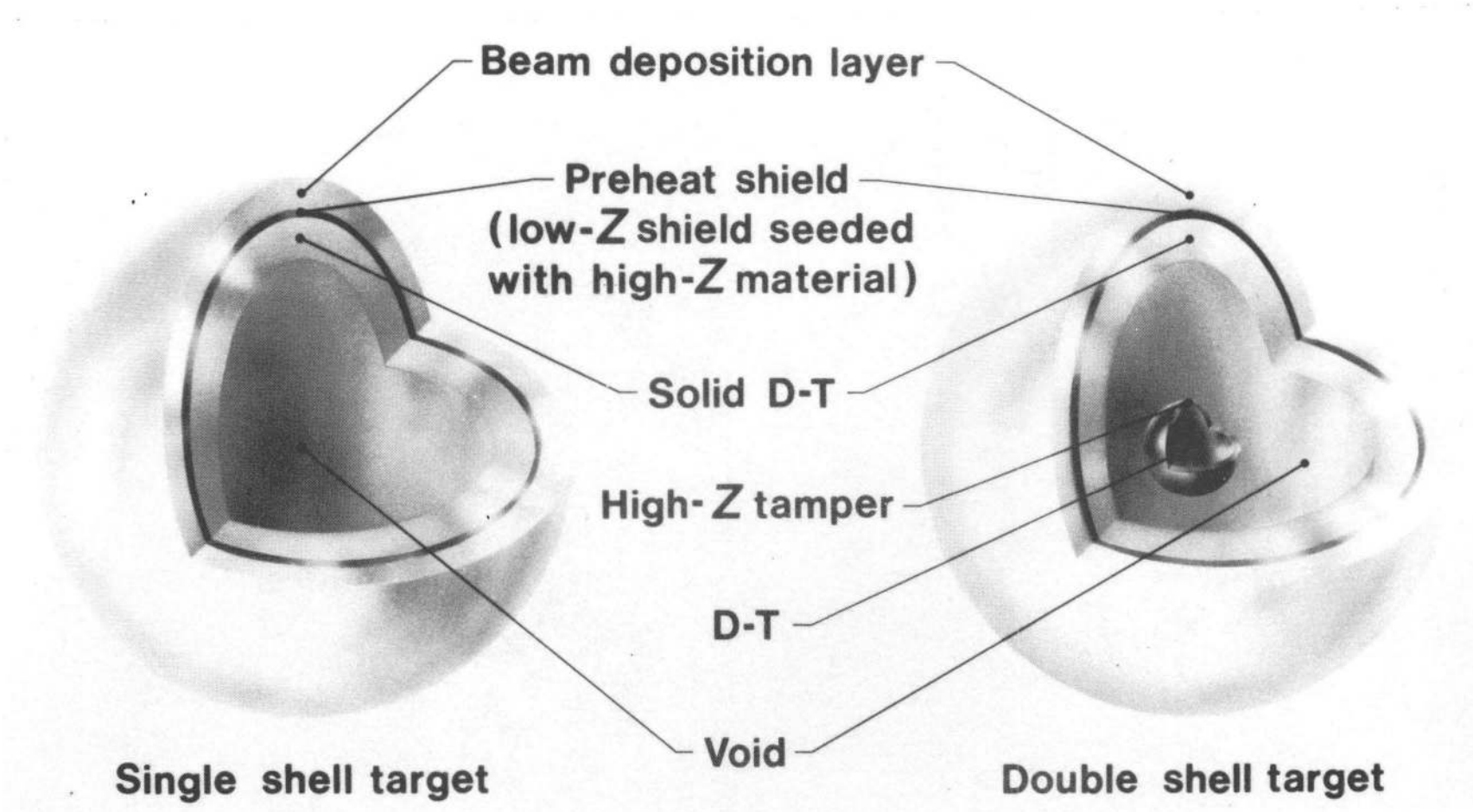

XBB 822-1494

Figure 2

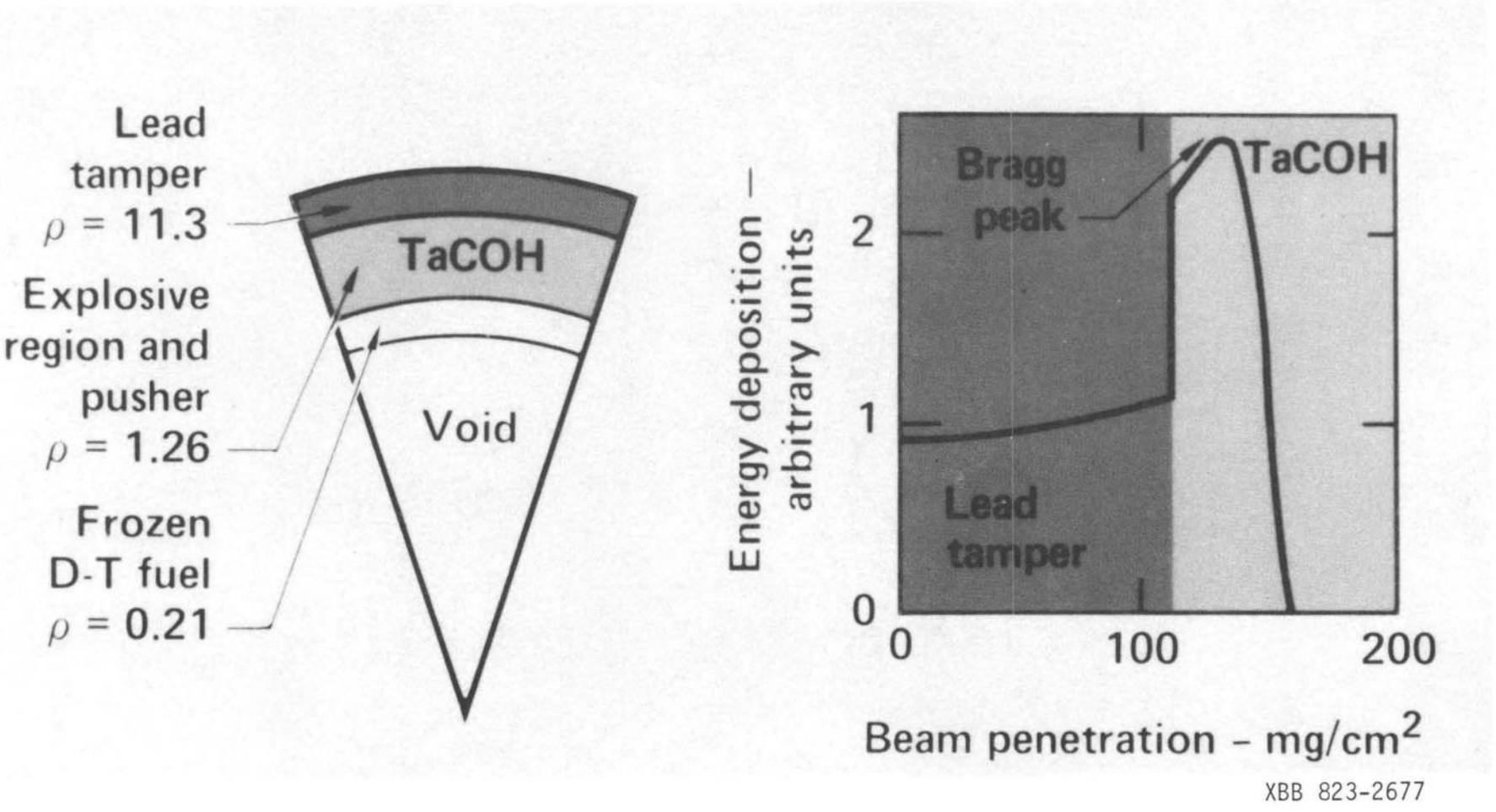
Lead
tamper
ρ = 11.3
Explosive
region and
pusher
ρ = 1.26
Frozen
D-T fuel
ρ = 0.21
TaCOH
Void
Energy deposition –
arbitrary units
Bragg
peak
TaCOH
Lead
tamper
0
1
2
0
100
200
Beam penetration – mg/cm²
XBB 823-2677

Figure 3

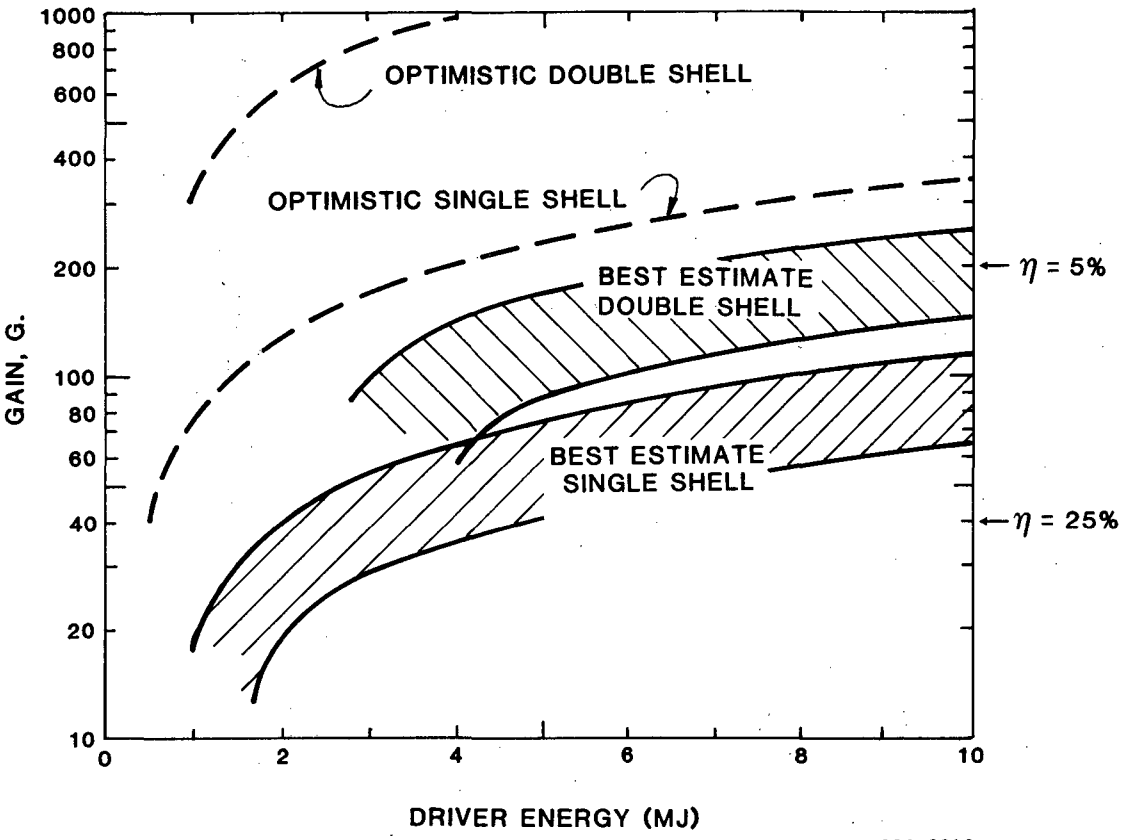
1000
800
600
400
200
100
80
60
40
20
10
GAIN, G.
OPTIMISTIC DOUBLE SHELL
OPTIMISTIC SINGLE SHELL
BEST ESTIMATE
DOUBLE SHELL
BEST ESTIMATE
SINGLE SHELL
← η = 5%
← η = 25%
0
2
4
6
8
10
DRIVER ENERGY (MJ)
XBL 823-8213

Figure 4

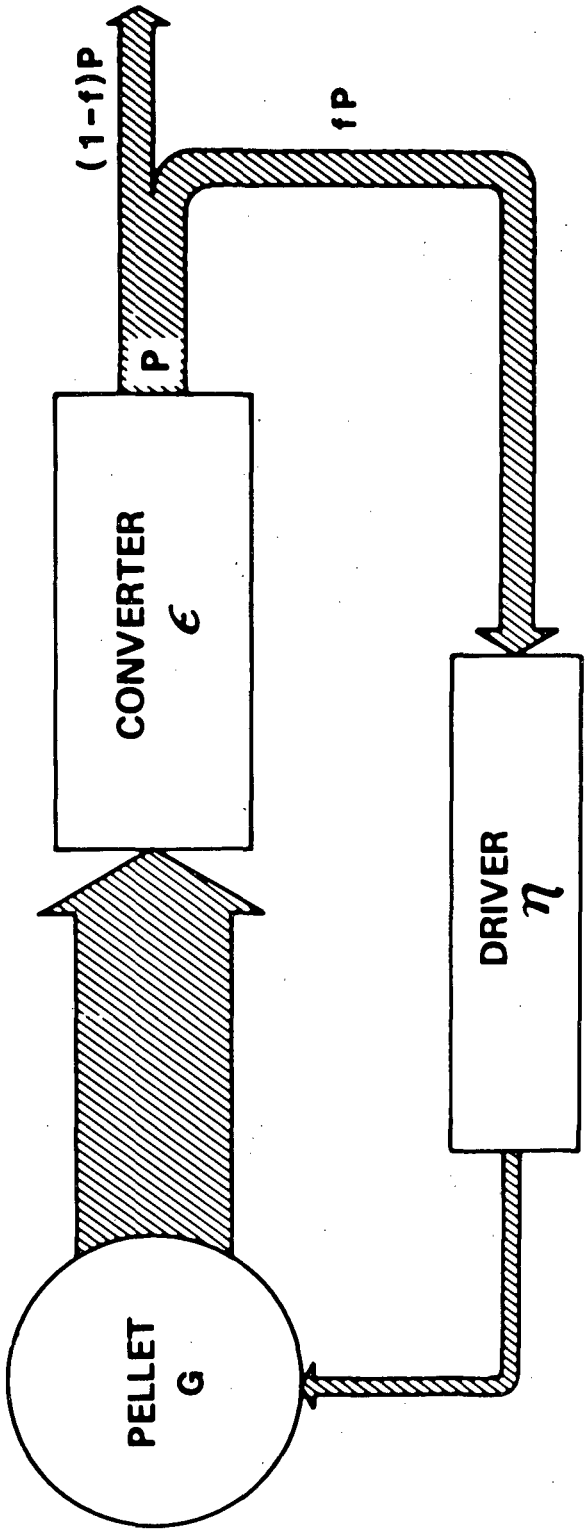

XBL 822-8072

Figure 5

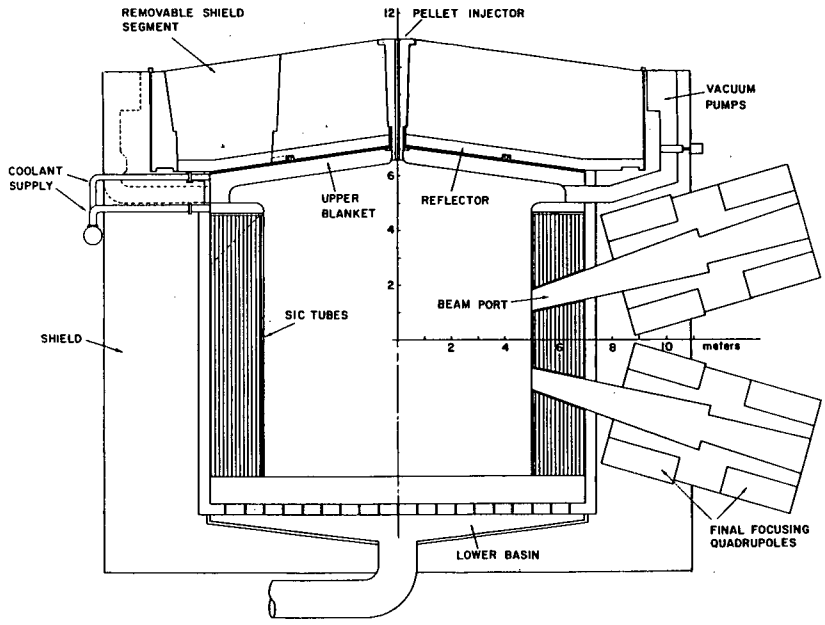
REMOVABLE SHIELD SEGMENT
PELLET INJECTOR
VACUUM PUMPS
COOLANT SUPPLY
UPPER BLANKET
REFLECTOR
BEAM PORT
SIC TUBES
SHIELD
meters
FINAL FOCUSING QUADRUPOLES
LOWER BASIN

Figure 6

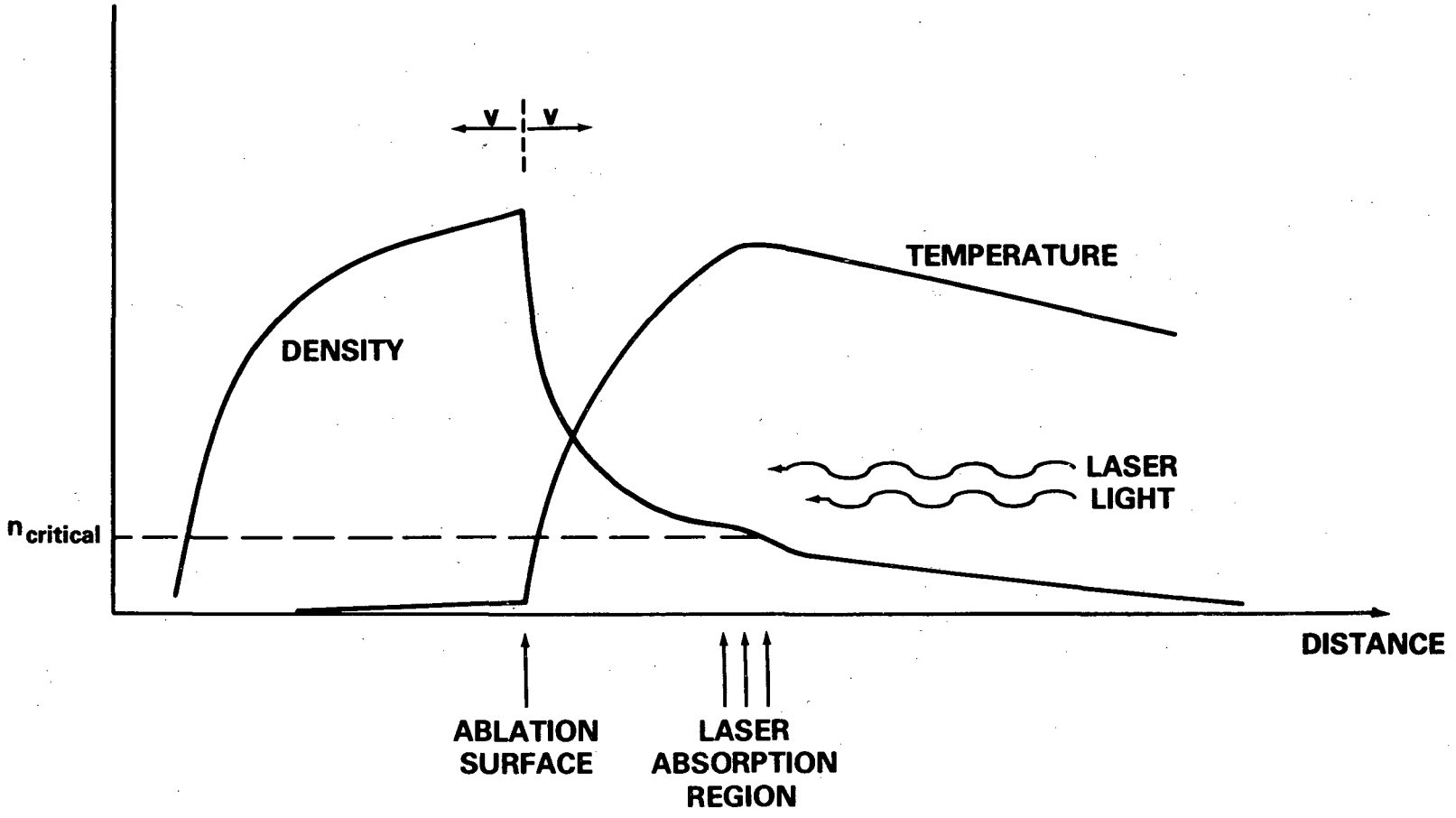
v
v
TEMPERATURE
DENSITY
LASER
LIGHT
$n_{critical}$
DISTANCE
ABLATION
SURFACE
LASER
ABSORPTION
REGION

Figure 7

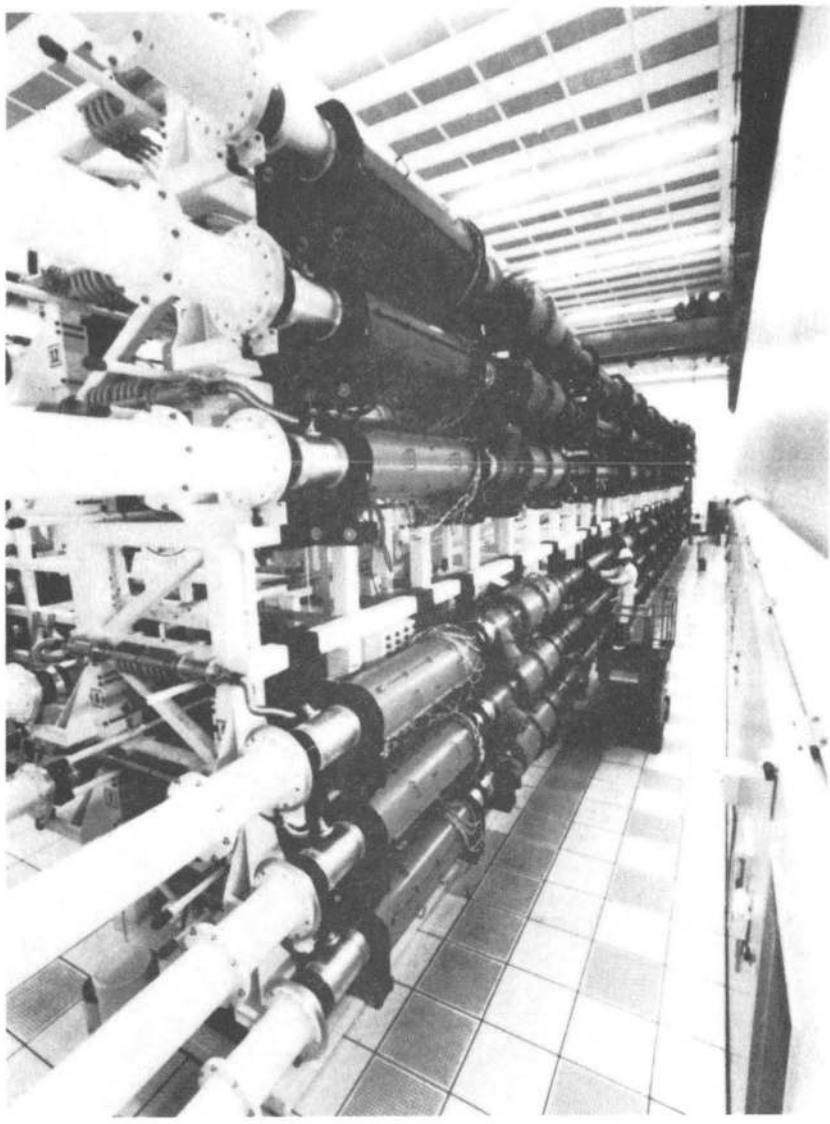

Figure 8

XBB 822-1493

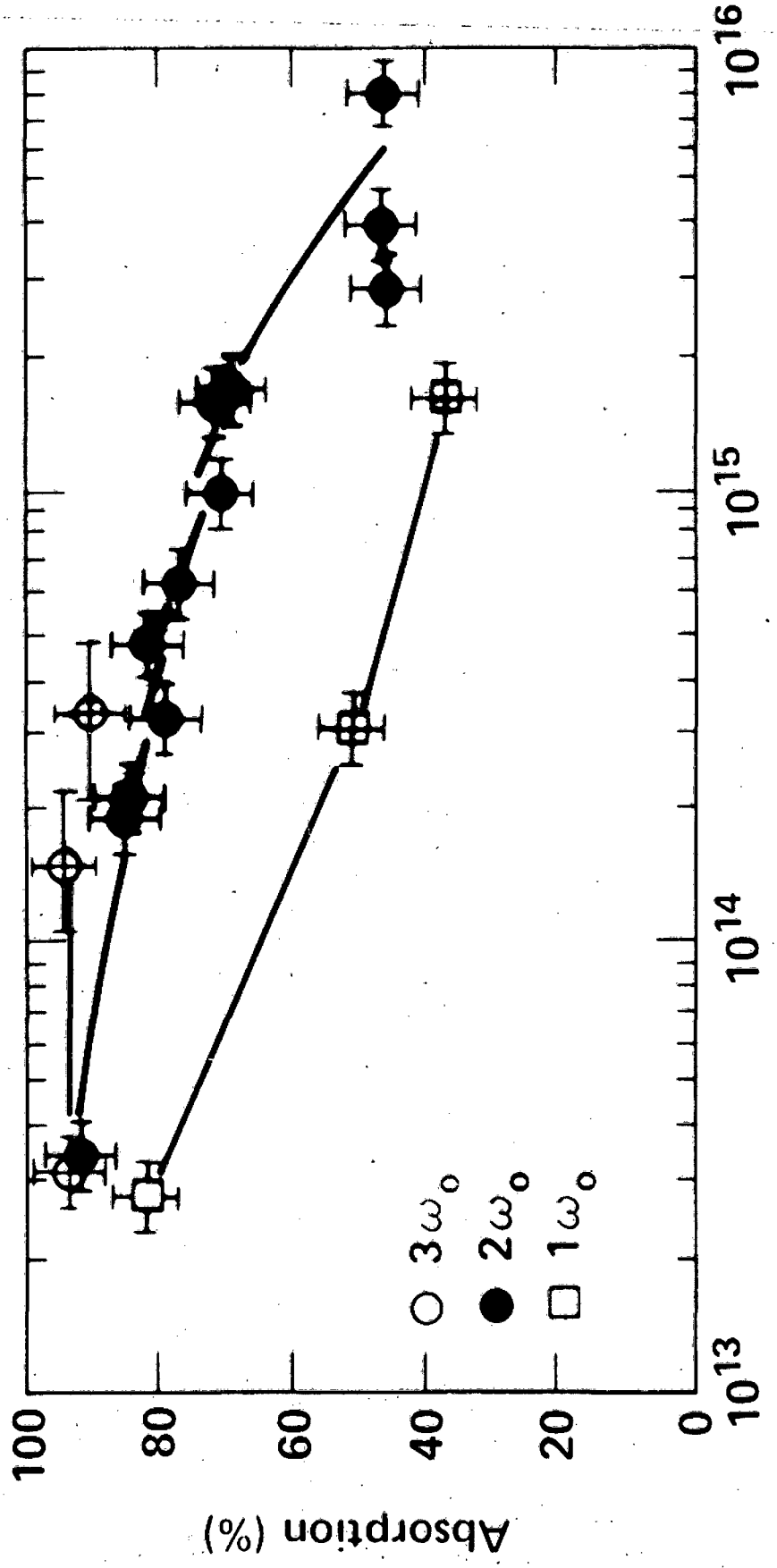

CBB 823-1841

Figure 9

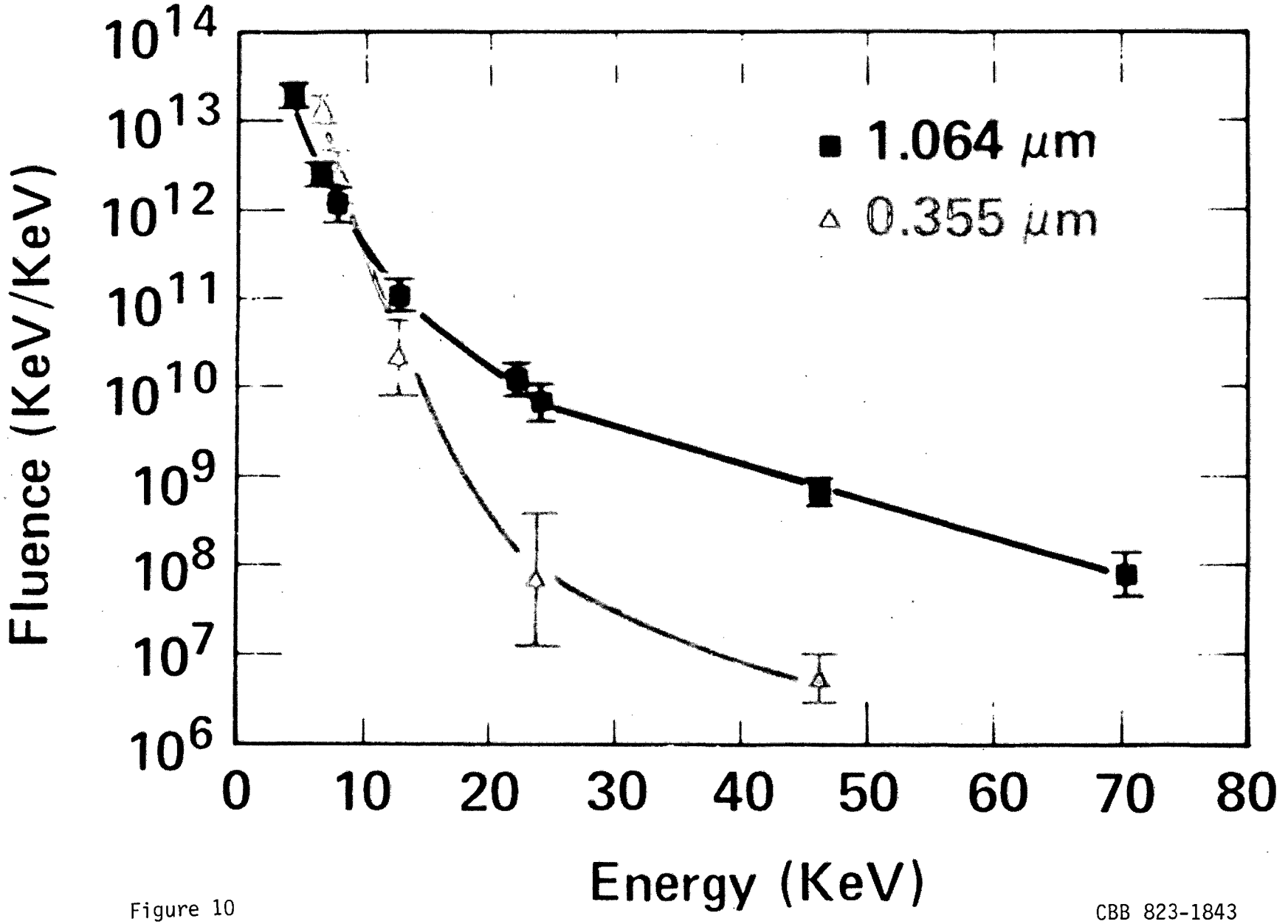

Figure 10

CBB 823-1843

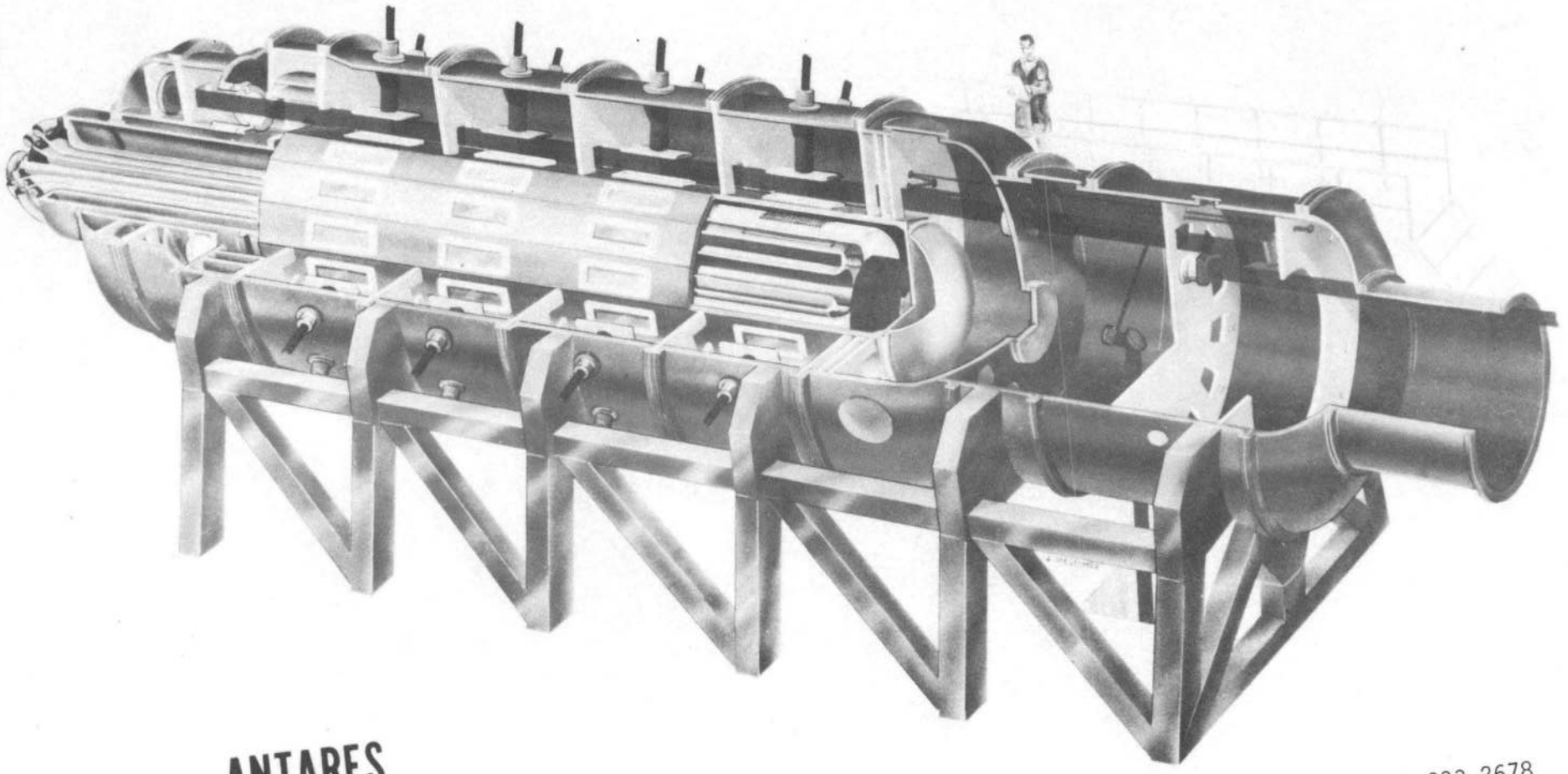

ANTARES

XBB 823-2678

Figure 11

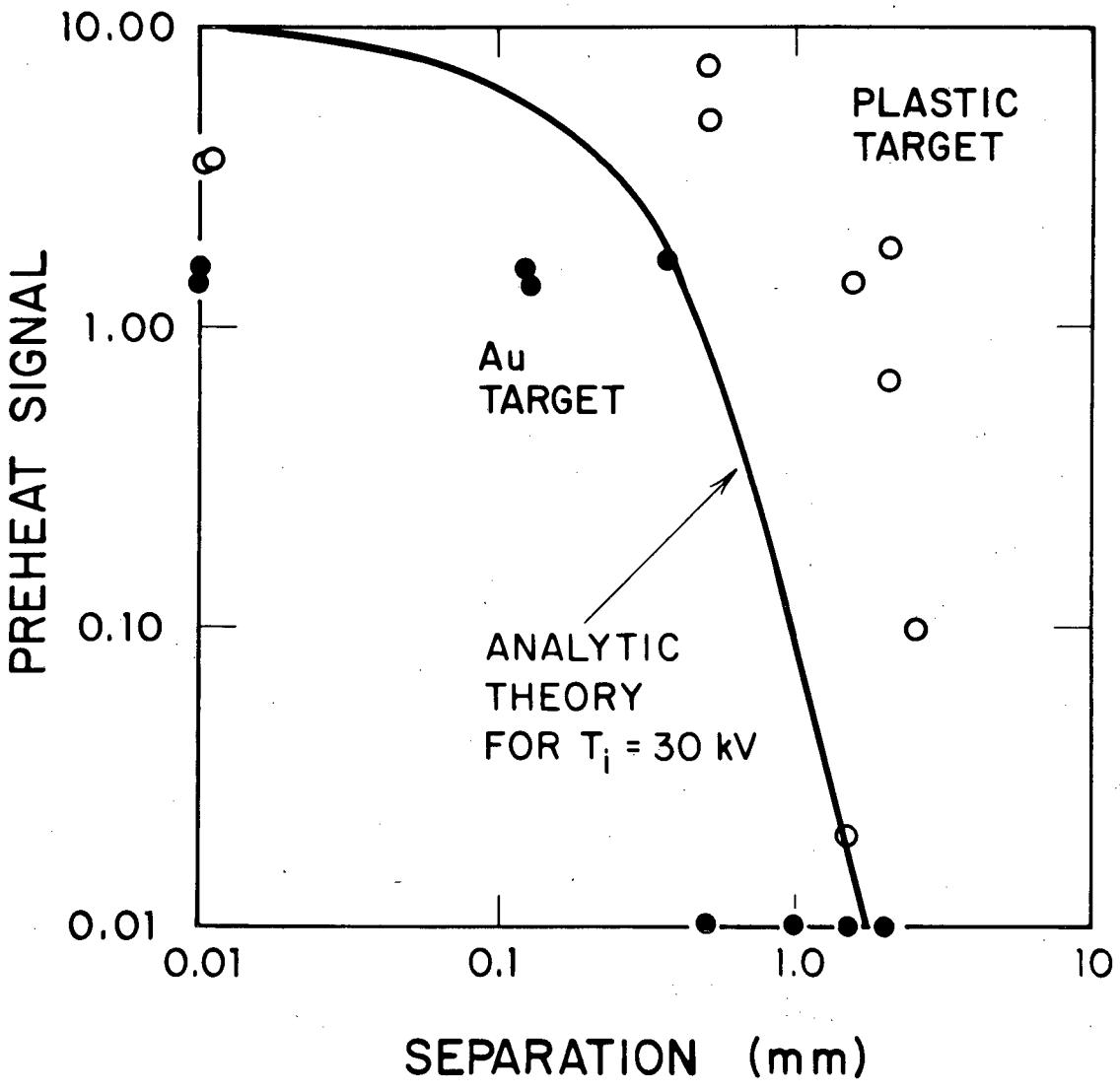

Figure 12

XBL 823-8489

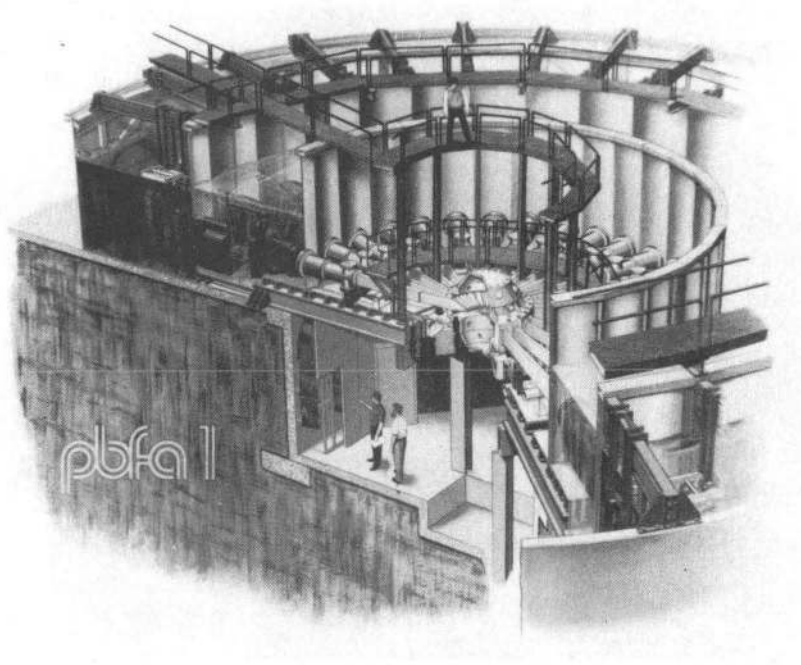

Figure 13

XBB 822-1479

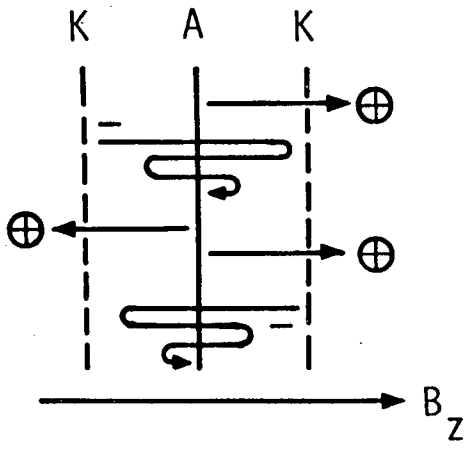

(a) Reflexing-electron

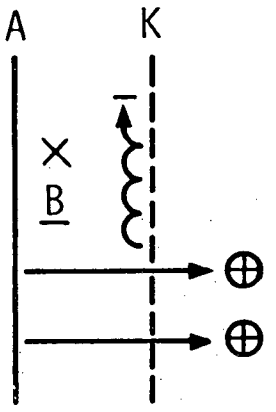

(b) Magnetically-insulated

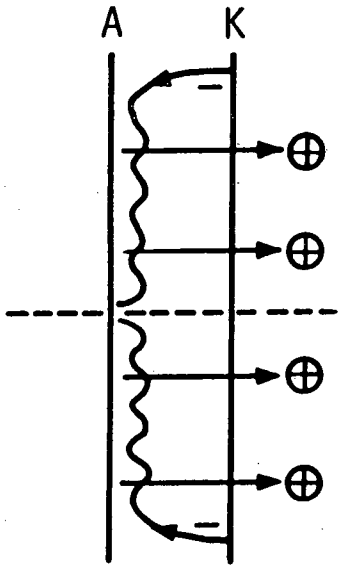

(c) Pinched electron beam

Figure 14

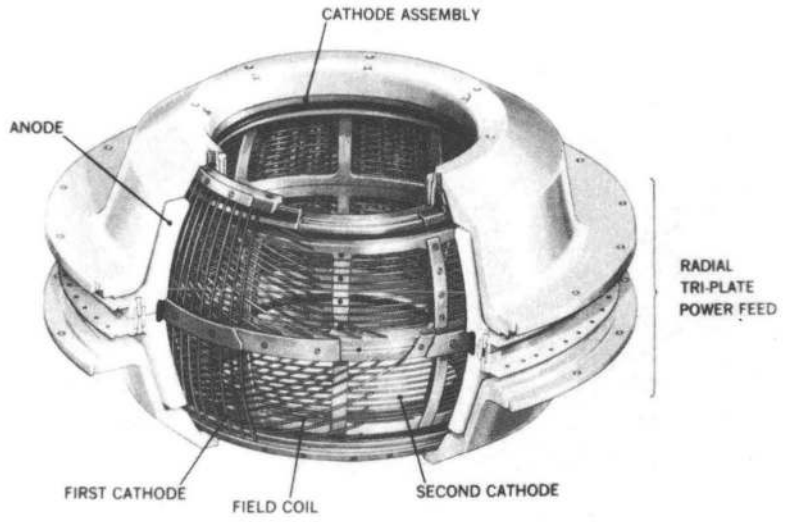

Figure 15 XBB 822-1478

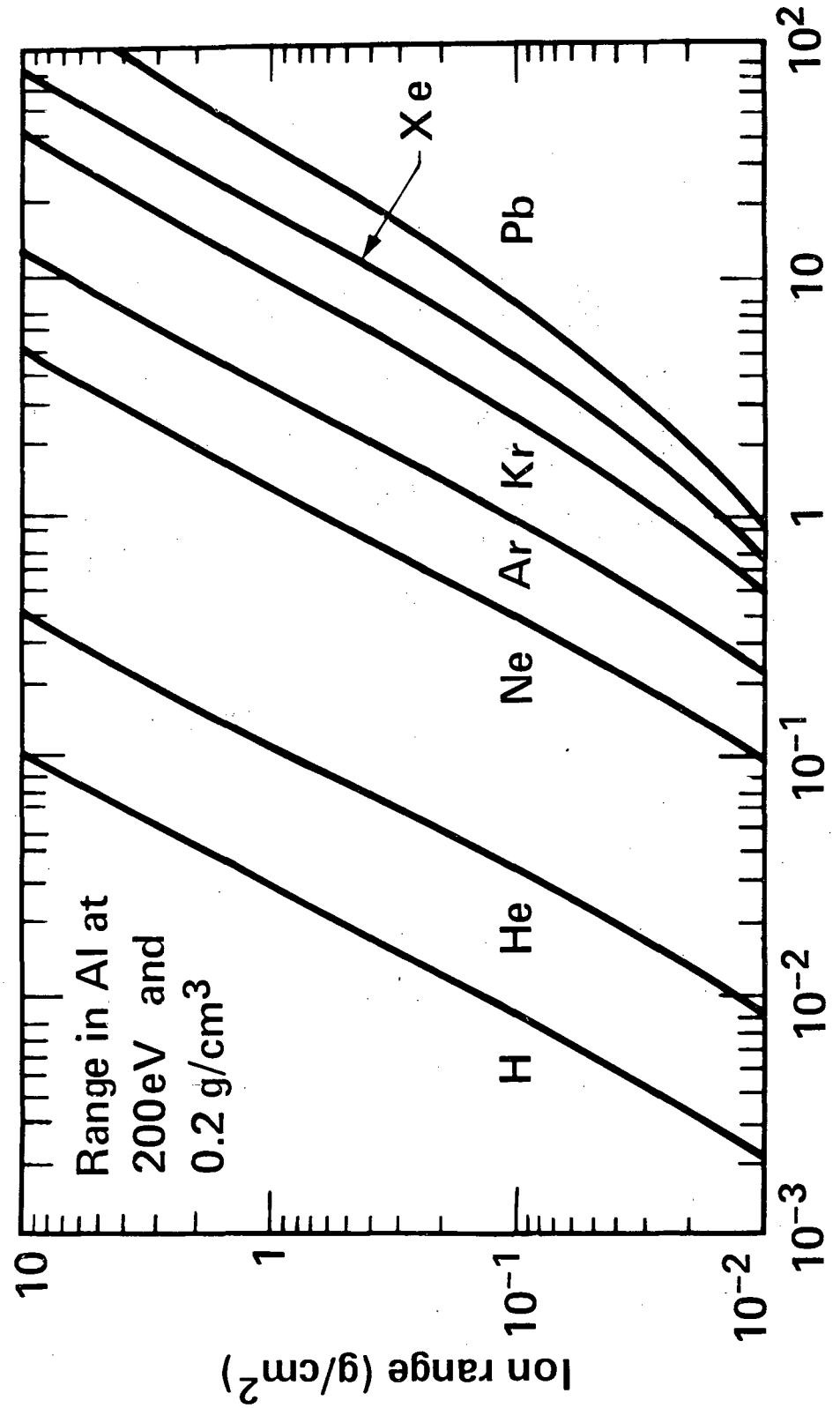
Ion range (g/cm²)
Ion energy (GeV)
Range in Al at
200eV and
0.2 g/cm³
H
He
Ne
Ar
Kr
Xe
Pb
10
1
10⁻¹
10⁻²
10⁻³
10⁻²
10⁻¹
1
10
10²

Figure 16

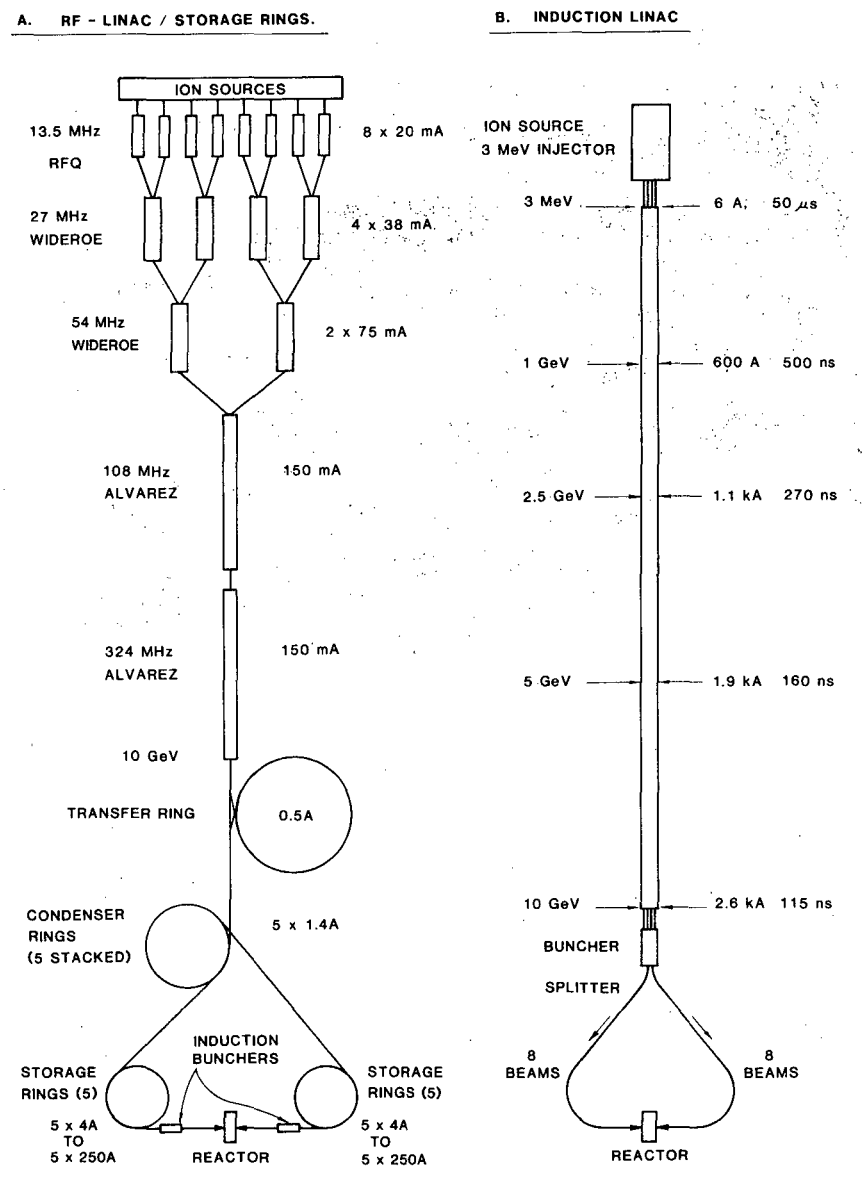
A. RF - LINAC / STORAGE RINGS.
ION SOURCES
13.5 MHz
RFQ
8 x 20 mA
27 MHz
WIDEROE
4 x 38 mA
54 MHz
WIDEROE
2 x 75 mA
108 MHz
ALVAREZ
150 mA
324 MHz
ALVAREZ
150 mA
10 GeV
TRANSFER RING
0.5A
CONDENSER
RINGS
(5 STACKED)
5 x 1.4A
INDUCTION
BUNCHERS
STORAGE
RINGS (5)
5 x 4A
TO
5 x 250A
REACTOR
STORAGE
RINGS (5)
5 x 4A
TO
5 x 250A
B. INDUCTION LINAC
ION SOURCE
3 MeV INJECTOR
3 MeV
6 A; 50 μs
1 GeV
600 A 500 ns
2.5 GeV
1.1 kA 270 ns
5 GeV
1.9 kA 160 ns
10 GeV
2.6 kA 115 ns
BUNCHER
SPLITTER
8
BEAMS
8
BEAMS
REACTOR

Figure 17

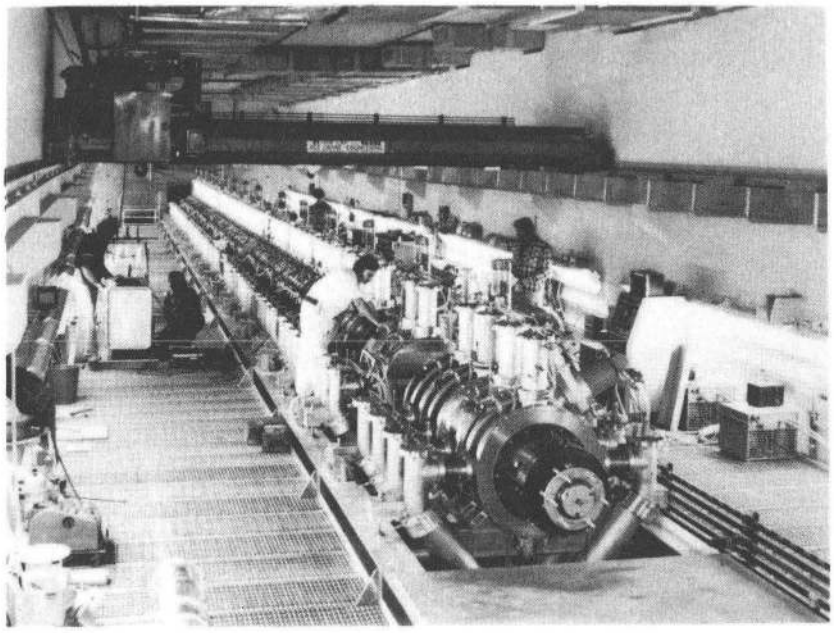

Figure 18 XBB 822-1477

Table 1 Fusion reactions

	Reaction energy (MeV)	Threshold plasma temperature (keV)	Maximum energy gain per fusion
$D + T \rightarrow {}^{4}He + N$	17.6	4	1800
$D + D \rightarrow {}^{3}He + N$	3.2	50	70
$D + D \rightarrow T + P$	4.0	50	80
$D + {}^{3}He \rightarrow {}^{4}He + P$	18.3	100	180
${}^{6}Li + P \rightarrow {}^{3}He + {}^{4}He$	4.0	900	6
${}^{6}Li + D \rightarrow {}^{7}Li + P$	5.0	>900	6
${}^{6}Li + D \rightarrow T + {}^{4}He + P$	2.6	>900	3
${}^{6}Li + D \rightarrow 2({}^{4}He)$	22.0	>900	22
${}^{7}Li + P \rightarrow 2({}^{4}He)$	17.5	>900	18
${}^{11}B + P \rightarrow 3({}^{4}He)$	8.7	300	30

Table 2 Driver requirements for power production

Energy - 1 to 10 MJ
Power - 100 to 600 TW
Pulse shape - control needed
(Driver efficiency) x (target gain) = $\eta G > 10$
Focusing - to a few millimeters at 5 to 10 m from the reactor wall
Reliability - > 80 percent on-time
Lifetime - 30 yrs
Repetition rate - 1 to 10 sec^{-1}
Cost - (a few) x 10^8 $ per GWe of electrical output

Table 3 Typical parameters for a ^{207}Pb ion-beam power plant driver

Beam energy	= 3 MJ/pulse
Ion kinetic energy	= 10 GeV (50 MeV/amu, $\beta = 0.3$)
Ion range	= 0.2 g/cm^2
Number of ions	= 2×10^{15}/pulse (300 particle μC)
Pulse length needed at target	= 20 nanoseconds
Power needed at target	= 150 TW
Beam current	= 15 kA
Focal spot radius	= 2.5 mm

TECHNICAL INFORMATION DEPARTMENT
LAWRENCE BERKELEY LABORATORY
UNIVERSITY OF CALIFORNIA
BERKELEY, CALIFORNIA 94720